T.R.
SİİRT UNIVERSITY
GRADUATE SCHOOL OF NATURAL AND APPLIED SCIENCES

INVESTIGATION OF THE EFFECT OF CURCUMIN ON HELICOBACTER PYLORI 5'-METHYLTHIOADENOSINE/S-ADENOSYLHOMOCYSTEINE NUCLEOSIDASE WITH MOLECULAR DYNAMICS METHOD

MASTER DEGREE THESIS

Student: MAHDI IBRAHIM SAEED
(163115004)

Department of Physics

Supervisor: Assoc. Prof. Ahmet YILDIRIM

September - 2018
SİİRT

THESIS ACCEPTANCE AND APPROVAL

The thesis entitled **"Investigation of the Effect of Curcumin on Helicobacter pylori 5'-methylthioadenosine/S-adenosylhomocysteine nucleosidase with Molecular Dynamics Method"** defended by Mahdi Ibrahim SAEED on 04/09/2018 has been approved as **Master Thesis** at Department of Physics, Graduate School of Natural and Applied Sciences, Siirt University with unanimity of votes by the committee listed below.

Jury Members	**Signature**
President- Supervisor Assoc. Prof. Ahmet YILDIRIM	.....
Member Asst. Prof. Cihat ÖZAYDIN	.....
Member Asst. Prof. Sabit HOROZ	.....

I approve the above results.

Assoc. Prof. Fevzi HANSU

Director, Graduate School of Natural and Applied Sciences

THESIS NOTIFICATION

This thesis, which is prepared in accordance with the thesis writing rules, complies with the scientific code of ethics, in case of exploitation of others' works it is referred to in accordance with the scientific norms, I declare that any part of the thesis that there is no tampering with the used data is not presented as another thesis work at this university or another university.

Signature

Mahdi Ibrahim SAEED

ACKNOWLEDGEMENT

I would like to express here my gratitude to my dissertation advisor, Assoc. Prof. Ahmet YILDIRIM, who supported me to accomplish this research, for his guidance and help during the time of this study, and for his patience, encouragement.

Special thanks go to Prof. Dr. Murat ERMAN President of University of Siirt for his help and support. Also, I thank to all Physics Department staff, who helped me to succeed in this work.

Finally, thanks to all my family members and friends for their help and encouragement to complete my study successfully.

Mahdi Ibrahim SAEED

SİİRT-2018

DEDICATION

To my parents.

To my sister and brothers.

To my wife for supporting me step by step.

To all of my children.

To all of my great teachers, who taught me and brought me up to this level.

CONTENTS

Page

LIST OF FIGURES

Page

ABBREVIATIONS LIST

Abbreviation	Explanation
MD	**:** Molecular dynamics
MTAN	**:** 5'-methylthioadenosine/S-adenosylhomocysteine nucleosidase
***Hp*MTAN**	**:** *Helicobacter pylori* 5'-methylthioadenosine/S-adenosylhomocysteine nucleosidase
MTA	**:** 5′-methylthioadenosine
SAH	**:** *S*-adenosylhomocysteine
LPO	**:** Lipid peroxid faction
V_{bond}	**:** Bond stretching potential
V_{angle}	**:** Angle potential
$V_{improper}$	**:** Proper dihedral potential
RMSD	**:** Root Mean Square Displacement
RMSF	**:** Root Mean Square Fluctuation
DCC	**:** Dynamical Cross-Correlation
LMI	**:** Linear Mutual Information
PME	**:** Particle-Mesh Ewald
DCCM	**:** Dynamical Cross-Correlation Map
GCM	**:** Generalized Correlation Map

Symbol	Explanation
nm	**:** nanometer
Å	**:** Angstrom
M	**:** Mol
α	**:** Alpha
β	**:** Beta
ns	**:** nanosecond
kcal	**:** kilocalorie
Σ	**:** Sum

ÖZET

YÜKSEK LİSANS TEZİ

KURKUMİNİN HELİKOBAKTER PİLORİ 5'-METHYLTHIOADENOSINE/S-ADENOSYLHOMOCYSTEINE NUCLEOSIDASE ÜZERİNE ETKİSİNİN MOLEKÜLER DİNAMİK YÖNTEMİ İLE İNCELENMESİ

Siirt Üniversitesi Fen Bilimleri Enstitüsü
Fizik Anabilim Dalı

Danışman: Doç. Dr. Ahmet YILDIRIM

2018, 48 Sayfa

Helikobakter pilori (*H. pilori*), gastrik ülsere ve mide enfeksiyonlarına neden olan bir bakteridir. *H. pilori*, metiyonin ve purin kurtarma yolları, futalosin yolu ve poliamin biyosentezi gibi çoğu bakteriyel metabolik işlemlerde 5′-methylthioadenosine/S-adenosylhomocysteine nucleosidase (MTAN) proteinine ihtiyaç duyar. MTAN proteini, bakteriyel metabolizmada ve bakteriler arası iletişimde önemli bir rol oynadığı için, *H. pilori* gelişimini önlemede önemli bir hedef inhibitör olabilir. Doğal bir bileşik olan kurkumin, *H. pilori* gelişimine karşı etkili bir inhibitör olarak varsayılabilir.

Bu çalışmada, Moleküler Dinamik simülasyon yöntemiyle *Hp*MTAN'ın konformasyonel yapısı ve dinamikleri üzerine kurkumin'in etkisini araştırdık. Kurkumin, *Hp*MTAN'ın tek bir zincirine ve her iki zincirine bağlıyken, *Hp*MTAN'ın davranışlarını karşılaştırdık. Elde edilen sonuçlara göre; kurkuminin yaklaşık olarak -8 kcal/mol'lük yüksek bir bağlanma enerjisiyle *Hp*MTAN'a bağlandığı ve aktif sitedeki bazı rezidülerle Hidrojen bağı oluşturduğu tespit edildi. Ayrıca, *Hp*MTAN'a kurkumin bağlanması büyük konformasyonel değişiklere ve rezidü dalgalanmalarına neden olmadığı ancak *Hp*MTAN'ın ara ve iç zincir korelasyonlarını arttırdığı gözlemlenmiştir.

Anahtar Kelimeler: Helikobakter pilori, Kurkumin, Moleküler dinamik, MTAN

ABSTRACT

MS THESIS

INVESTIGATION OF THE EFFECT OF CURCUMIN ON HELICOBACTER PYLORI 5'-METHYLTHIOADENOSINE/S-ADENOSYLHOMOCYSTEINE NUCLEOSIDASE WITH MOLECULAR DYNAMICS METHOD

Mahdi Ibrahim SAEED
The Graduate School of Natural and Applied Science of Siirt University
The Degree of Master of Science
In Physics Science

Supervisor: Assoc. Prof. Ahmet YILDIRIM

2018, 48 Pages

Helicobacter pylori (*H. pylori*) is a bacteria that causes gastric ulcers and stomach infections. *H. pylori* requires the protein 5′ -methylthioadenosine/S-adenosylhomocysteine nucleosidase (MTAN) for many bacterial metabolic processes including the methionine and purine salvage pathways, the futalosine pathway, and polyamine biosynthesis. Since MTAN plays an important role in bacterial metabolism and communication, it can be an important inhibitor target to prevent *H. pylori* growth. A natural compound curcumin can be considered as potent inhibitor against *H. pylori* growth.

In this study, we investigated the effect of curcumin on the conformational structure and dynamics of *Hp*MTAN using Molecular Dynamics simulations. We compared the behavior of *Hp*MTAN when curcumin is bound to single and both chain(s) of *Hp*MTAN. Our results reveal that curcumin has a high binding energy of around -8 kcal/mol with *Hp*MTAN and forms Hydrogen bonds with some active site residues. In addition, it was observed that curcumin binding to *Hp*MTAN does not cause large conformational changes and large residue fluctuations, however, it arises both inter and intra chain correlations of *Hp*MTAN.

Keywords: Curcumin, Helicobacter pylori, Molecular dynamics, MTAN

1. INTRODUCTION

In 1982, Australian scientists Robin Warren and Barry Marshall reported the existence of Helicobacter pylori (*H. pylori*) bacteria in gastric ulcers and stomach infections. It was not previously known as *H. pylori* but was called Campylobacter pylori. *H. pylori* is a helix shaped and gram-negative bacterium. Many studies revealed that *H. pylori* infection can cause many diseases including gastritis (Dooley et al., 1988) and peptic ulcer (Kashiwagi, 2003). *H. pylori* requires the protein 5′-methylthioadenosine/S-adenosylhomocysteine nucleosidase (MTAN) for many important bacterial metabolic processes such as the purine and methionine salvage pathways, the futalosine pathway, and polyamine biosynthesis (Li et al. 2011; Mishra and Ronning 2012; Ronning et al. 2010). However, to our knowledge, no extensive investigation on the conformational structure and dynamics of *H. pylori* MTAN (*Hp*MTAN) has been yet performed with Molecular Dynamics (MD) simulations.

MD simulation is a computer simulation method for studying the physical motions of atoms in a protein or protein-ligand complex. In a biological system, the interactions between the atoms or residues of the protein can be simulated with molecular mechanics simulations. MD simulation provides information on the time dependent behavior of a molecular system and allows for the investigation into the conformational and dynamical changes of the molecular system during simulation time. MD simulations have become an important tool for understanding the protein molecules and their interactions with other small/large molecules and the importance of natural products in drug discovery during last few decades.

In recent years, many researchers have focused on natural anti-inflammatory agents such as curcumin and sulphorane (Maroon et al., 2010). They also reported from some experimental studies that curcumin might have antimicrobial, anti-cancer, anti-inflammatory and antioxidant effects. Therefore, it is crucial to understand the inhibitory and other effects of curcumin on the protein molecules. In this study, we investigated the effect of curcumin on the conformational structure and dynamics of *Hp*MTAN using MD simulations. We compared the behavior of *Hp*MTAN when curcumin is bound to single chain and both chains compare with unligated *Hp*MTAN.

2. LITERATURE REVIEW

Over three decades have passed since the primary discovery of *H. pylori* by two Australians, Warren and Marshall (1988). Helicobacter pylori is a Gram-negative bacterium that causes gastric ulcers and stomach infections. *H. pylori* contamination was distinguished as a significant factor in numerous illnesses, including peptic ulcer, gastritis and many gastric malignancies (Kashiwagi, 2003; Dooley et al., 1989; Plummer et al., 2004). In spite of the fact that contamination rate is falling in developed nations (Sipponen, 1997), it is still high in developing countries (Bardhan, 1997). *H. pylori* is identified with 85% of gastric and 95% of duodenal ulcers diseases and is a critical hazard factor for gastric malignancies (De Falcoet al., 2015; Kuipers, 1995). *H. pylori* is generally seen in asymptomatic people with healthy stomachs, proposing that the bacterium is the stomach commensally.

Previous investigations have noted that gastritis tends to increment with going older (Siurala et al., 1968; Ihamaki et al., 1979; Villako et al., 1976; Correa et al., 1976). Similar patterns have been seen for *H. pylori* contamination that utilized indirect strategies for evaluation (Graham et al., 1988; Kaldor et al., 1986; Jones et al., 1986).

H. pylori is vulnerable to a wide range of antimicrobial medicine (McNulty et al., 1985). However, a small numbers are active in vivo (Marshall et al., 1988; McNulty et al., 1986). A significant age tendency for the prevalence's of *H. pylori* disease and gastritis were found in the subjects who had not utilised either anti-biotics or bismuth.

Numerous methods are accessible for the analysis of *H. pylori* disease in gastric biopsy specimens (Dooley, 1988). The detection of *H. pylori* by culture is the most precise method, but it has a tendency to be insensitive. The histological stain is the strategy utilized most generally for the determination of *H. pylori* infection. A few studies advise the routine hematoxylin-eosinstain, while other suggests the warthin - Starry silver stain (Marshall et al., 1988) or the Giemsa stain (Paull, 1988).

Antibiotic treatments for *H. pylori* disease turned out to be further difficult, with even triple and fourfold treatments being regularly unsuccessful as medication resistance has developed (Selgrad, 2011). Modern antibiotics agents are required for *H. pylori* diseases with novel targets and systems of activity.

Recently, Li et al., 2011, established that *Hp*MTAN proteins perform a crucial part in another possible menaquinone biosynthetic pathway. They revealed that, not at all like E. coli and T. thermophillus, C. jejuni and *H. pylori* biosynthesize menaquinone

though an in-between step that needs MTAN to catalyse the hydrolysis of 6-amino-6-deoxyfutalosine. These tasks imply that MTAN represents an objective for mixes fit for influencing bacterial digestion and bacterial correspondence (Parveen, 2011; Hiratsuka et al., 2008; Seto et al., 2008). Indeed, recently, Wang et al 2012, revealed that influential inhibitors of MTAN inhibit the development of *H. pylori*.

The bacterial MTANs are double substrate compounds hydrolyzing 5′-methylthioadenosine (MTA) and *S*-adenosylhomocysteine (SAH) to produce 5-methylthioribose or *S*-ribosylhomocysteine, and adenine. In most microscopic organisms, MTAN is associated with methionine reusing, quorum sensing and polyamine synthesis, but is not critical for cell survival or growth (Miller, 2001; Parveen, N., 2011, Gutierrez et al., 2009). The multi-functionality of MTAN arises because of its substrate promiscuity, which puts MTAN at the central point of a scope of metabolic procedures.

Bacteria usually communicate with each other in their atmosphere through a system called “quorum sensing” (Fuqua et al., 1994). Numerous exercises, for instance biofilm development, symbiosis, and virulence, antibiotic generation, are controlled by quorum sensing systems (Miller and Bassler, 2001).

Menaquinone is a block imposed on this pathway and crucial for electron movement in the maturities of gram-positive and anaerobic gram-negative bacteria by inhibition of the MTANs would likely be deadly to the organisms (Suttie, 2009; Popp et al., 1989; Kurosu, 2010).

An examined has been done on the adaptation and dynamics of holo and apo *Hp*MTAN and evaluated the impact of protonation of residue aspartate 198 (D198), which is the active site of MTAN is by all accounts of significant importance, by performing as a hydrogen-bond acceptor for the ligand by utilization of molecular dynamics simulations. The outcomes demonstrate that protonation of the active site of HpMTAN can cause a conformational change from a closed state to an open state even without substrate, through interchange mechanical coupling (Tekpinar et al., 2015).

MTAN is a promising inhibitor target (Schramm, 2007; Gutierrez et al., 2009) since it is exogenous to people and is essential in bacterial digestion and correspondence, it has been demonstrated that inhibition of MTAN can prevent development of *H. pylori* (Mishra and Ronning 2013; Wang et al., 2012). This has prompted various structural examinations on MTANs in various living beings (Bao et al., 2013; Gutierrez et al. 2009; Haapalainen et al., 2013).

An exceptional feature of MTANs is their homo-dimer structure. *Hp*MTAN likewise isn't a special case, and each chain of *Hp*MTAN has ten strand β-sheets, six α-helices and a solitary 3_{10} helix. Of these, α helix 6 close to the active site is of significant importance. In the closed shape, the helix has a fold from residues 203 – 211, which transforms into a loop in MTAN's open frame. Another remarkable feature is an D198 residue which is saved across numerous species such as E. coli, S. aureus, S. pneumoniae, H. influenzae, S. typhimurium, M. tuberculosis, T. pallidum, and *H. pylori* (Lee et al., 2003).

D198 is placed in the active site of HpMTAN, close to α-helix 6. It has been suggested that D198 behaves as a proton donor, and its protonation states are fundamental in the course of catalysis. Transfer of a proton from D198 residue to the N7 residue position of the adenine ring leads to de-linking of the N-glycosidic bond (Appleby et al., 1999; Lee et al., 2001). Finally, adenine ring gives back its proton to D198 residue. These occasions bring up an intriguing issue with respect to the impact of protonation on the structure and dynamics of HpMTAN and its catalytic part (Wang et al., 2014). Both ligand binding and protonation processes could cause dynamic site opening by various mechanisms.

On the other hand, valuable immunization for *H. pylori* has not been accomplished in people yet (Rad et al., 2007). In this sense, it is necessary to discover alternative treatments, especially identified with nourishment, for example, plant extract that contain various polyphenols, which have appeared to diminish infection (Bengmark et al., 2009). Various investigations have stated that curcumin has an extensive variety of biological effects including antimicrobial, cancer prevention agent, and antitumor (Ruby et al., 1995). Likewise, curcumin has some immunosuppressive applications (Gao et al., 2004). Including appearance of cytokines, for example, IL-1 and TNF-α (Chan M., 1995; Moon D., 2006). Then again, curcumin improved phagocytise action of macrophages. Many of bacterial cells in the contaminated creature stomach demonstrated that curcumin supplementation diminished the whole amount of *H. pylori* (Vetvicka et al., 2016). A mouse investigation demonstrated that orally-given curcumin caused critical restraint of gastric infection brought by *H. pylori* disease (Santos et al., 2015).

Long period in vivo or pre-clinical examinations are either less or not that much successful (Di Mario et al., 2007). Low dissolvability, poor absorption and less bio-availability are likely the key reasons behind this inadequacy. Since curcumin is useful

against *H. pylori* impact, extra examinations are important to build up curcumin as a simple medicinal answer for a possibly problematical infections (Sarkar, 2016).

Previous reports have demonstrated that curcumin can obstruct NF-κB actuation in *H. pylori*-contaminated gastric epithelial cells in vivo mouse case (Foryst-Ludwing et al., 2004). The assessment demonstrated that curcumin was compelling in diminishing the irritation of the gastric mucosa of *H. pylori*-infected mice, which was affirmed (Santos et al., 2015).

Additionally late investigation in rats utilizing histology and in human being, serology, showed that treatment with curcumin completely enhanced gastric inflammation related with *H. pylori* disease regardless of persistence of the bacterium, supporting the discoveries of this examination (Sintara et al., 2015; Di Mario et al., 2007). Nevertheless, these information are not affirmed (Kundu et al., 2011) that recommended the curcumin acted two courses amid insurance against *H. pylori* disease, by destroying *H. pylori* and in addition possibly focusing on molecules engaged in the *H. pylori*-brought gastric diseases as proposed by Goel and coworkers (Goel et al., 2008).

There are two primary approaches by which *H. pylori* may cause gastric irritation. Initially, the organism might interact with surface epithelial cells, delivering either cell harm or the freedom of epithelial-inferred chemokines. The epithelial chemokine reaction might be especially essential in the beginning times of *H. pylori*-prompted inflammation, with the epithelium acting as a pivotal first line of protection against microbial disease. Secondly, *H. pylori*-inferred items may access the beneath mucosa, accordingly straight forwardly invigorating host non-particular and particular immune responses involving the release of a range of cytokine messengers (Bodger, 1998).

3. MATERIALS AND METHODS

3.1. Protein

A protein molecule is a very large and complex molecule that play many critical roles in the alive body. The majority of the work in cells is done by proteins and they are required for the structure, function, and the body's tissues and organ's regulation.

3.1.1. Amino acid

Proteins consist of many smaller units called amino acids, which make long chains by attaching each one to another. Amino acids are defined as organic compounds and they contain both a carboxyl as well as an amine group (Figure 3.1).

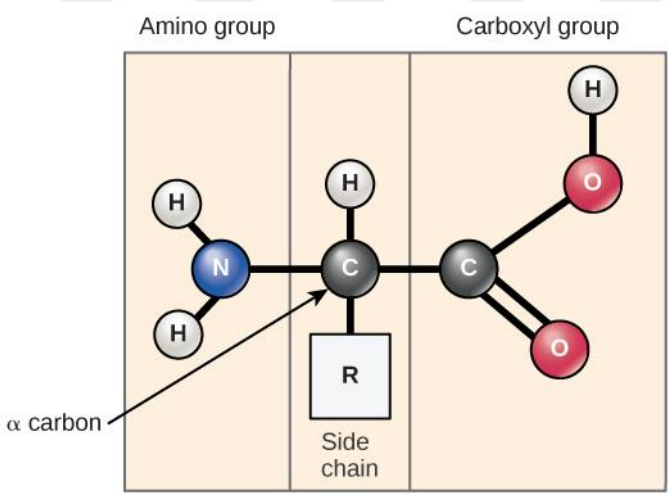

Figure 3.1. Amino acid structure (Anonymous, 2018a).

The amino acids have around 20 natural types (Figure 3.2). The combination of these amino acids make a protein and their sequences determine the protein's structure and function.

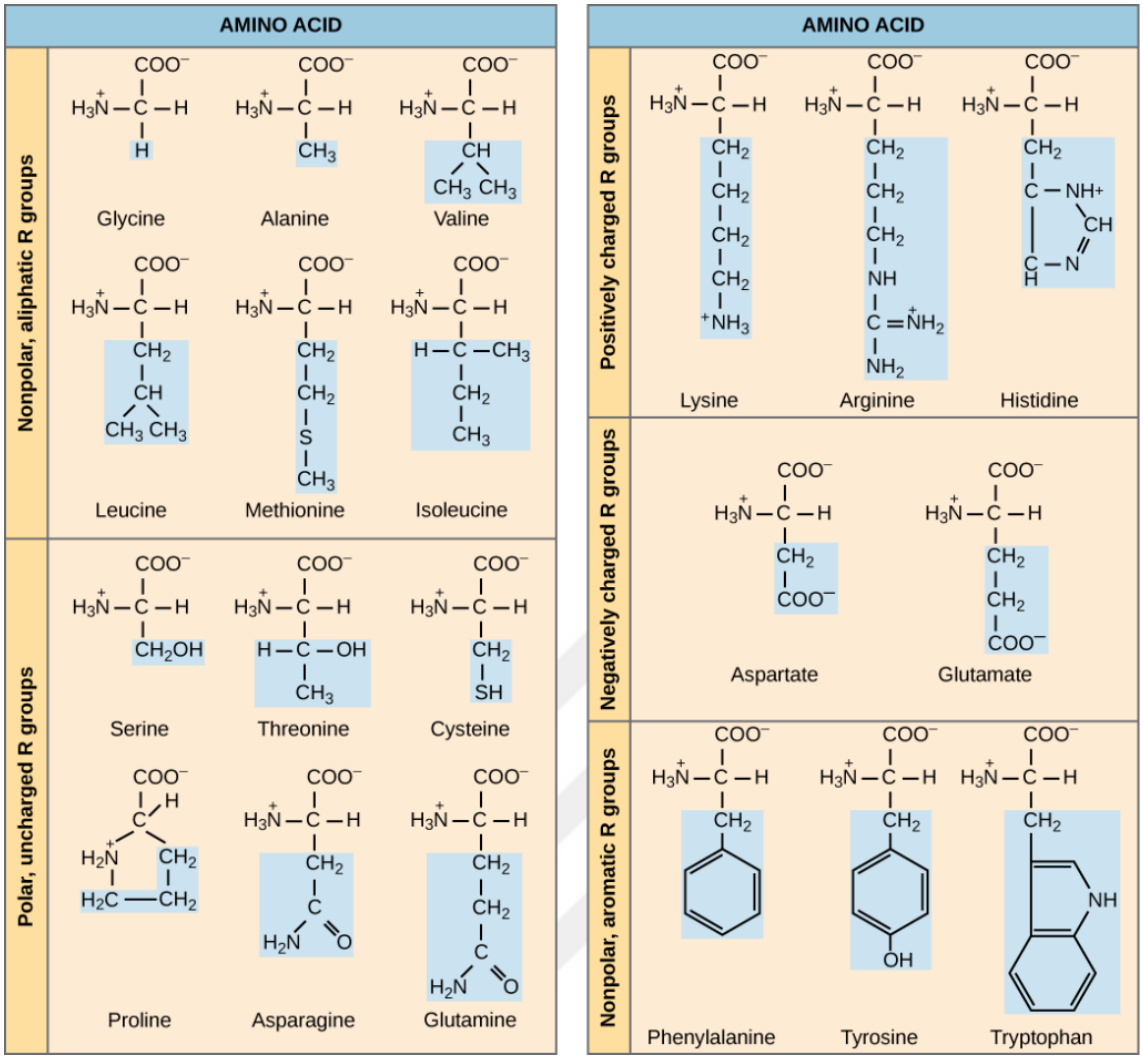

Figure 3.2. 20 standard amino acids (Anonymous, 2018a).

3.1.2. Protein Structure and Function

The three-dimensional structure of a protein is represented by its amino acid sequence. Amino acids forming protein are attached to one another with a peptide bond. To perform their biological function in biological systems, proteins fold into one or more specific spatial conformations via non-covalent interactions such as hydrophobic bonds, hydrogen bonds, ionic bonds and Van der Waals interactions.

The size of protein structures vary from tens to thousand amino acids (Brocchier, 2005). The protein sizes are physically classified as nano particles because their sizes are between 1–100 nm.

A protein may go through reversible structural changes to perform its biological function. The modified structures of the same protein are called as different

conformations, and transitions between them are known as conformational changes. Protein structure has four levels, which are primary, secondary, tertiary, and quaternary structure (Richardson, 1981).

The linear sequence of amino acids in the polypeptide chain is called protein primary structure (Figure 3.3). The primary structure is usually formed by covalent bonds, which are made through the procedure of protein biosynthesis.

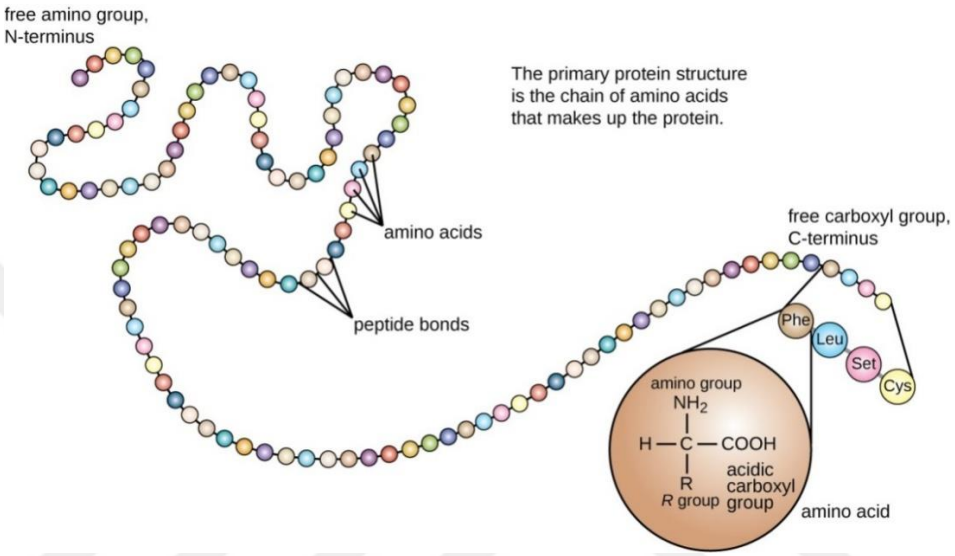

Figure 3.3. The primary structure of a protein (Anonymous, 2018b).

The secondary structure emerges after synthesis; when polypeptide chains of a protein are folded or pleated into different shapes (Figure 3.4). α-helices and β-sheets are the most famous secondary structural elements. In additional to them, there are turns, bends and coils but they are less structured motifs. Hydrogen bond is the main bond in a secondary structure, which allow holding together, overall giving the shape great stability.

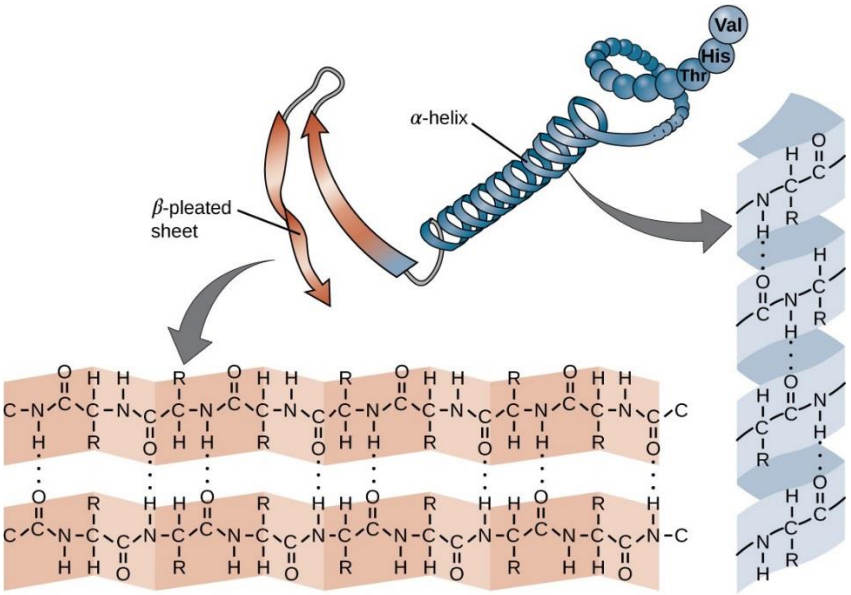

Figure 3.4. The secondary structure of a protein (Anonymous, 2018b).

Tertiary structure; the three-dimensional structure of a protein, entailing and shaping of a several secondary structure is tertiary structure, which holds together by four different bonds and interactions (Figure (3.5). In these structures, besides to hydrogen bonding, amino acid side chains of the several secondary structures initiate to interact with each other in various techniques, such as ionic interactions, hydrophobic interactions, and disulfide bonds (Bromberg and Dill, 1994).

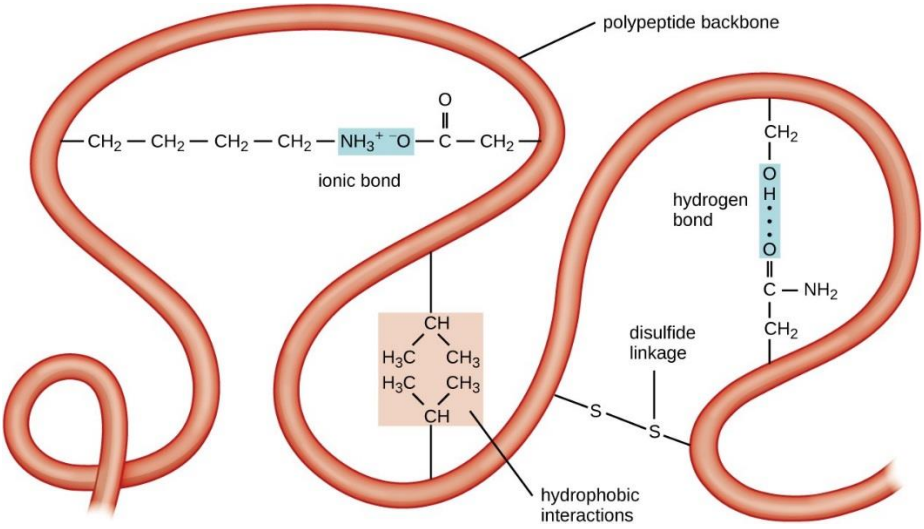

Figure 3.5. The tertiary structure of a protein (Anonymous, 2018b).

Quaternary structure of a protein is a shaped one by two or more polypeptide chains linked together to form a multi-subunit complex (Figure 3.6). Frequently, a

protein may be composed of a couple of polymer chains, each one with its very own tertiary structure. Positions of those chains with respect to each other establish quaternary protein structure (Dill et al., 1995).

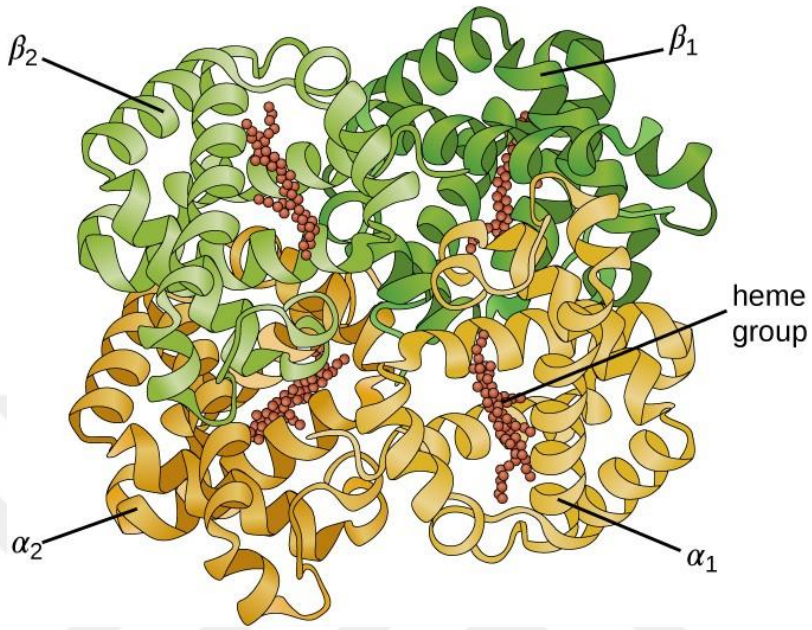

Figure 3.6. The quaternary structure of a protein (Anonymous, 2018b).

3.1.3. Ligand

Ligand refers to an ion and a molecule that binds to a biomolecule to form a complex structure. Ligand binding to a receptor protein changes the chemical conformation by affecting the 3-dimensional structure of the receptor. Ligands include substrates, inhibitors, activators, and neurotransmitters. In DNA-ligand complex studies, the ligand can be a small molecule, ion (Teif, 2005) or protein (Teif, 2010) which binds to the double helix of DNA.

The strength of binding is known as affinity, and describes a tendency or strength of the impact. Binding affinity is completed now not simplest by means of host-guest interactions, but additionally by way of solvent effects, which have a dominant and steric role forming non-covalent binding in solution (Baron, 2010).

3.1.4. Curcumin

Curcumin is one of three curcuminoids group in turmeric, which are natural phenols in charge of turmeric's yellow color (Figure 3.7). It is recognized to have numerous pharmacologic properties and is broadly utilized as a herbal medicine, for instance, for peptic diseases in ayurvedic medicine (Balachandran et al., 2005). It is red at basic pH and strongly yellow at acidic pH. This sparingly water dissolvable and lipophilic particle have two perfumed rings associated by two unsaturated carbonyl gatherings. The particle is balanced out by hydrogen bond with the focal hydroxyl group (Surth, 2002; Kewitz et al., 2013).

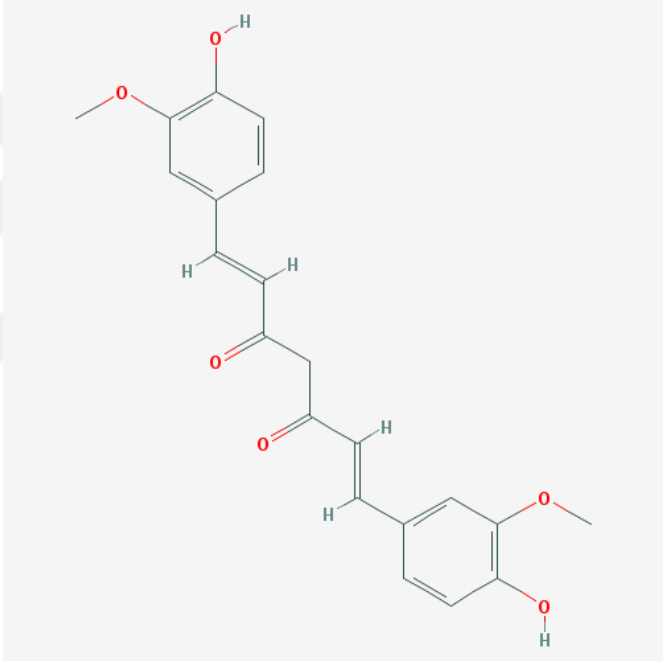

Figure 3.7. Chemical structure of curcumin (Kim et al., 2015).

3.1.5. Protein-ligand complex

Protein-ligand interactions play an important role in controlling of cellular processes such as assembly of organelles, enzyme catalysis, signaling, expression, diverse control functions, energy transduction, replication and storage of the genetic material. In addition, protein-ligand interactions are responsible for the mechanism of many medicine therapies. A schematic diagram for a protein-ligand complex is given in Figure 3.8.

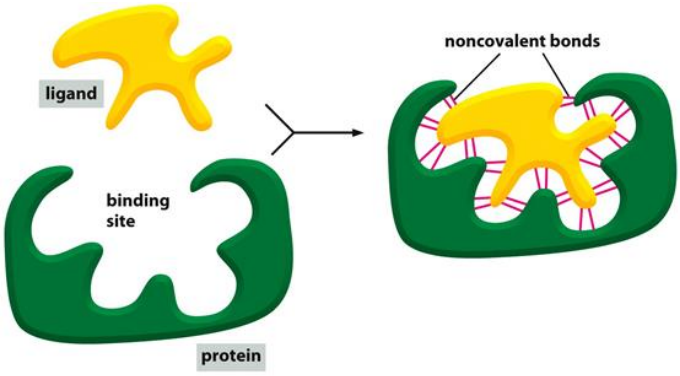

Figure 3.8. A schematic diagram of a protein-ligand complex (Anonymous, 2018c).

3.1.6. Helicobacter pylori 5'-methylthioadenosine/S-adenosyl homocysteine nucleosidase

H. pylori is a type of bacteria that is responsible for around 90% of gastric and duodenal ulcer sickness. It is also an important risk factor for gastric malignancies (De Falco et al., 2015; Kuipers, 1995). *H. pylori* needs the protein MTAN for many bacterial metabolic processes including the methionine and purine salvage pathways, the futalosine pathway, and polyamine biosynthesis (Li et al., 2011; Mishra and Ronning 2012; Ronning et al., 2010).

In addition to bacterial metabolic processes, MTAN is involved in the quorum sensing of a number of bacterial species and *H. pylori* is one of them. Quorum sensing controls many activities such as antibiotic production, biofilm formation, symbiosis and virulence (Miller and Bassler, 2001).

Since MTAN plays an important role in bacterial metabolism and communication, it can be an important inhibitor target to prevent *H. pylori* growth (Mishra and Ronning 2013; Wang et al., 2012). Even though there are several experimental studies on *Hp*MTAN, to our knowledge, no extensive investigation on interactions of *Hp*MTAN with curcumin has been performed with MD simulations.

The crystal structure of MTAN is a homo-dimer structure and each chain of MTAN consists of ten strand β-sheets, a single 3_{10}-helix, and six α-helices (Figure 3.9).

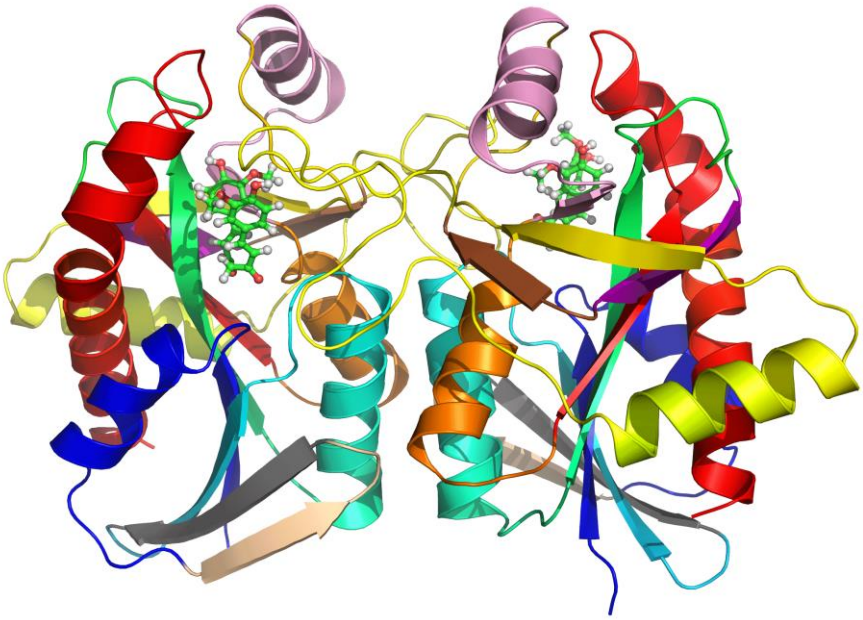

Figure 3.9. *Hp*MTAN-curcumin complex.

3.2. Molecular Dynamics Simulations

MD simulation is a computer simulation method that provides detailed information on the physical motions of atoms and/or residues within a biological molecule such as protein and nucleic acid. MD calculates the time dependent behavior of a molecular system and can provide not only detailed information on the fluctuations and conformational changes of the system but also an accurate estimation of the binding free energy of the protein-ligand interactions. Thus, MD simulations have become an essential technique for drug-design studies.

In MD simulations, the Newton's equation of motion is used to calculate the time evolution of a system. The trajectories corresponding to the dynamical motions of the atoms in the system are obtained from the simulation. The trajectory file consists of a sequence of coordinate frames that contain the time varying atomic coordinates for the system during the simulation. Each set of coordinates is defined as one frame in time. Therefore, a trajectory allows for the investigation into the conformational and dynamical changes of the system over time. The basic MD algorithm is given in Figure 3.10.

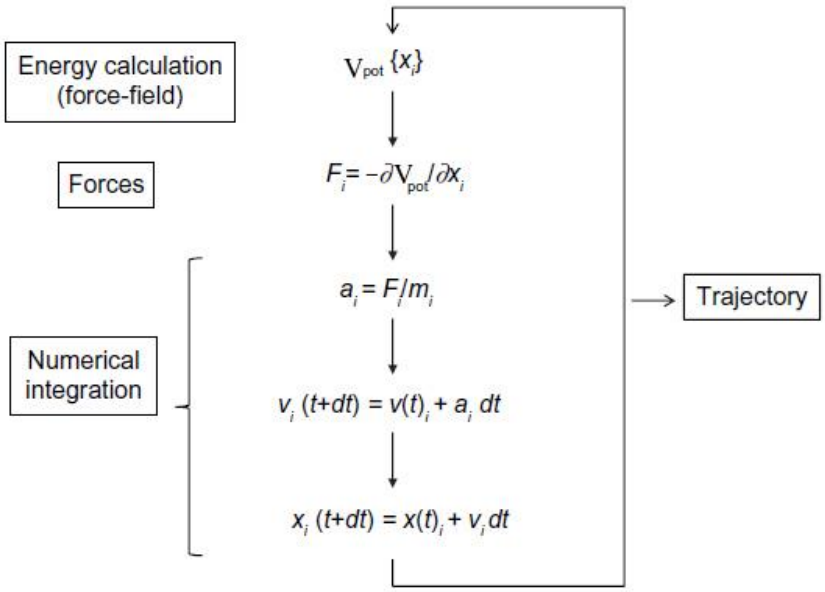

Figure 3.10. Molecular dynamics basic algorithm (Hospital et al., 2005).

3.2.1. Equations of motion

MD simulation method in physical perspective is based on the equations of motion which comes from solution of Newton's second law. Just by knowing the force on each atom, the velocity, acceleration, and position of each atom in the system can easily be found. By integrating of the Newton's second law then yields a trajectory which brings up to the velocities as well as positions and accelerations of the particles accordingly to the time change. Using MD simulations and by repeating small time step femtosecond iterations millions of times, dynamics of solvated proteins are measured up to the hundreds of nanosecond time scale.

Newton's second law or the equation of motion is given by

$$F_i = m_i a_i \tag{3.1}$$

where F_i is the force exerted on particle i, m_i is the mass of particle i and a_i is the acceleration of particle i. Negative gradient of a conservative potential V equals to the force for each atom (Eq. 3.2)

$$\vec{F} = -\vec{\nabla} V \tag{3.2}$$

These two equations are united to yield

$$-\frac{dV}{dr_i} = m_i \frac{d^2 r_i}{dt^2} \tag{3.3}$$

where r_i is the position of atom i. As seen from Eq. 3.3, one needs potential (force field) to calculate the time development of acceleration, velocities and positions of a molecule.

3.2.2. Force Field

MD simulation consists of the numerical solution of the traditional equations of motion. For this purpose, the force acting on the atoms is required which can be derived from a potential energy function. The potential energy function is also known as force field. The force field is broken down into terms characterizing diverse types of interactions in a bimolecular system. These interactions can be divided into two general categories: non-bonded interactions and bonded interactions.

Bonded interaction contains the proper dihedral, bond, angle and improper dihedral interaction terms (Figure 3.11).

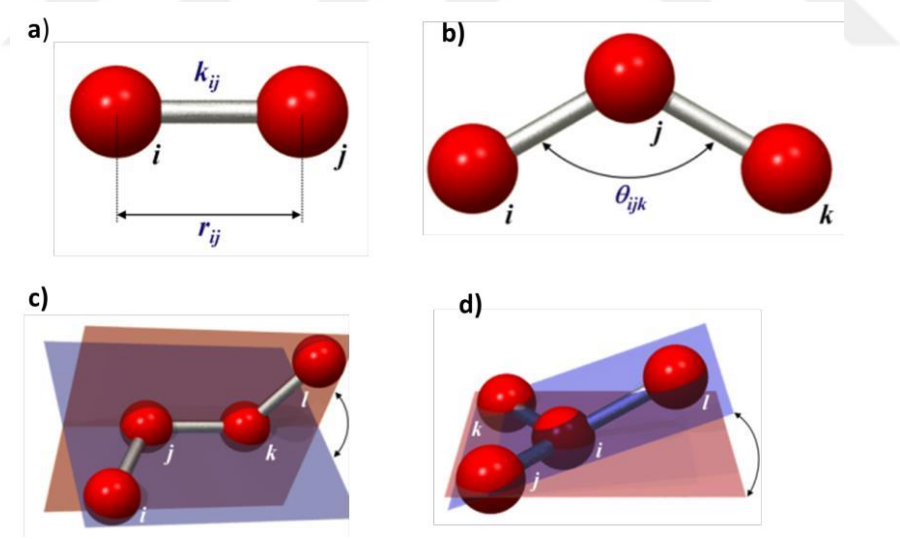

Figure 3.11. Bonded interactions, a) Bond, b) Angle, c) Proper dihedral and d) Improper dihedral (Kouza, 2013).

Bond stretching potential:

$$V_{bond} = k_b(b + b_0)^2 \tag{3.4}$$

where k_b is force constant of bond, b is the length of the bond between two atoms, and b_0 is the equilibrium bond length between two atoms.

Angle potential:

$$V_{angle} = k_\theta(\theta + \theta_0)^2 \tag{3.5}$$

where k_θ is force constant of angle, θ is the angle between two atoms, and θ_0 is the equilibrium angle between two atoms. However, dihedral potentials are categorized into two types.

Proper dihedral potential:

Proper dihedral potential depends on the interactions of four consecutive bonded atoms. The contributions of torsional angle changes to the potential energy of the system are calculated by equation 3.6 (Figure 3.11.c)

$$V_{improper} = k_\emptyset[1 + \cos(n\emptyset - \delta)] \tag{3.6}$$

where $k_\emptyset$ is proper dihedral force constant, θ is current the torsion angle, n is multiplicity or the periodicity of the rotation (the number of cycles per 360^o rotation about the dihedral), and δ is an phase angle for the dihedral angle that defines minimum energy.

Improper dihedral potential:

Improper dihedral potential, which is used to force atoms to keep in a plain, is based on quartet atoms as proper dihedral and given by three atoms centered around a fourth atom (Figure 3.11.d).

$$V_{improper} = k_\psi(\psi + \psi_0)^2 \tag{3.7}$$

where k_ψ, $\psi$and ψ_0 are force constant, instantaneous and equilibrium improper dihedral angle, respectively.

Non-bonded interactions consist of the Van der Waals and electrostatic interaction terms.

Van der Waals potential:

Van der Waals or Lennard-Jones potential (Jones, 1924) describes the interaction between two non-bonded atoms. It is given by

$$V_{LJ} = 4\varepsilon\left[\left(\frac{\sigma}{r}\right)^{12} - \left(\frac{\sigma}{r}\right)^{6}\right] = \varepsilon[\left(\frac{r_m}{r}\right)^{12} - 2\left(\frac{r_m}{r}\right)^{6}] \quad (3.8)$$

where ε is a parameter characterizing the depth of the potential well and a measure of how strongly the two particles attract each other, σ is refers to the minimal distance between the interacting particles, where potential equals to zero. r is the distance from any atom to any other atom in the simulation and r_m is the distance, where the potential reach a minimum ($-\varepsilon$) when $r_m = 2^{1/6}\sigma \approx 1.122\sigma$.

The first term of Van der Waals potential, which is repulsive term, is due to the overlap of the molecular orbitals (Pauli repulsion) at short ranges. The second term refers to attraction at long ranges.

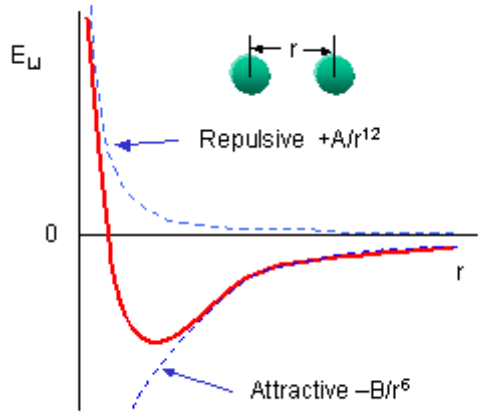

Figure 3.12. Van der Waals potential (Anonymous, 2018d).

Coulomb potential:

Coulomb potential describes the potential energy of interaction between two charged atoms.

$$V_{elec} = \sum_{ij} \frac{q_i q_j}{4\pi\varepsilon_0 r_{ij}} \quad (3.9)$$

where q_i and q_j are the partial charges of atom $i$and j respectively, ε_0 is the permittivity of vacuum, and r_{ij}indicate the distance between atoms i and j.

The total potential energy of a molecular system, which is the sum of bonded and non-bonded energy terms, defines the molecular mechanical force field and given by

$$V = V_{bond} + V_{angle} + V_{dihedral} + V_{improper} + V_{vdw} + V_{elec} \quad (3.10)$$

The functional forms of molecular mechanical force fields are similar to Eq. 3.10 but the force constants, Van der Waals parameters and partial charge assignment for the different force fields may differ (Wang and McCammon, 2012). The force fields commonly used in molecular modeling of biological macromolecules are AMBER (Cornell et al., 1995), Charmm (MacKerell et al., 1998), GROMOS (Oostenbrink et al., 2004) and OPLS (Jorgensen, et al., 1996).

3.2.3. Analysis of trajectories

To investigate conformational and dynamical properties of the systems studied we performed the analyses below by using the trajectories obtained from MD simulations.

3.2.3.1. Root Mean Square Displacement (RMSD)

The RMSD is the measure of the average change in displacement of certain atoms for a particular frame in a molecule with respect to a reference frame (mostly initial frame) after roto-translational least-squares fitting to a reference frame. It is expressed as

$$RMSD(t) = \sqrt{\frac{1}{N}\sum_{i=1}^{N}(r_i^{\text{ref}} - r_i(\text{t}))^2} \quad (3.11)$$

Here, N is the number of atoms (in our case only $C\alpha$ atoms), r_i^{ref} is the position of i^{th} reference $C\alpha$ atom and $r_i(\text{t})$ is the position of $C\alpha$ atom i at time t.

3.2.3.2. Root Mean Square Fluctuation (RMSF)

The flexibility of residues in the protein can be measured by RMSF by aligning each snapshot (frame) to the average structure of the protein. RMSF is defined by

$$RMSF(i) = \sqrt{\frac{1}{T}\sum_{t=1}^{T}(r_i(\mathrm{t}) - \langle r_i \rangle)^2} \quad (3.12)$$

where r_i is the position of i^{th}atom, $\langle r_i \rangle$ refers to the average position of r_i during simulation time and T is the number of total frames in simulation.

3.2.3.3. Dynamical Cross-Correlations

Dynamical cross-correlation (DCC) between $i^{th}(r_i)$ and $j^{th}(r_j)$ residues can be calculated from a set of frames (t_n) of a trajectory after fitting to a reference frame as defined by the following equation,

$$DCC_{ij} = \langle \Delta r_i \cdot \Delta r_j \rangle = \frac{1}{T}\sum_{n}^{T} \Delta r_i(t_n) \cdot \Delta r_j(t_n) \quad (3.13)$$

where T is the number of total frames in simulation. The normalized DCCs (nDCCs) is defined as

$$nDCC_{ij} = \frac{DCC_{ij}}{[DCC_{ii}DCC_{jj}]^{1/2}} \quad (3.14)$$

nDCC varies between [-1,1], where -1 refers to a fully anticorrelated motion between $C\alpha$ atoms of two residues (i.e. motion in opposite direction), 0 indicates no correlation and 1 refers to a fully correlated motion. We used Bio3D package to calculate nDCCs from MD trajectories (Grant, 2006).

3.2.3.4. Linear mutual information

LMI is another useful method to calculate motional correlations between residue pairs. LMI values vary from 0 to 1. 0indicates no correlation while 1 indicates complete correlation. LMI can be calculated as follows (Lange and Grubmuller, 2006):

$$LMI_{ij} = \frac{1}{2}\left[\ln(\det C_i) + \ln(\det C_j) - \ln(\det C_{ij})\right] \quad (3.15)$$

Here, $C_i = \langle x_i^T x_i \rangle$ and $C_{ij} = \langle (x_i, x_j)^T (x_i, x_j)) \rangle$ while $x_i = r_i - \langle r_i \rangle$. r_i represents position vector of atom i. We used g_correlation program to calculate linear and generalized correlations of each system based on the LMI (Lange and Grubmuller, 2006).

It should be noted that correlations between perpendicular motions are captured by the LMI but not the DCC method. Anticorrelations between residue pairs are not estimated by the LMI method.

3.2.4. Simulation details

Experimental *Hp*MTAN complex was obtained from the Protein Data Bank (Westbrook et al, 2002) under accession code 4WKP (Wang et al, 2015) All MD simulations were carried out using the MD software package GROMACS (Lindahl et al, 2011) with a leap-frog stochastic dynamics integrator (van Gunsteren and Berendsen, 1990), AMBER99SB-ILDN force field (Lindorff-Larsen et al, 2010), TIP3P water model (Jorgensen et al., 1983), LINCS algorithm (Hess et al., 1997) for bond constraints. The energy minimization was performed using the steepest descent algorithm. The solvation procedure carried out using a layer of at least 1.2 nm between the box edge and the solutes, in a rhombic dodecahedron box for periodic boundary conditions. The ion concentration of 0.15 M NaCl was applied to neutralize the systems and obtain physiologically relevant salt concentrations. The Parrinello-Rahman barostat (Parrinello and Rahman, 1981) was employed to maintain a pressure of 1 bar with coupling time of 0.1 ps and a compressibility of 4.5×10^{-5} bar. The temperature was coupled to 300 K, using the V-rescale thermostat (Bussi et al., 2007) with a coupling constant of 0.1 ps. The particle-mesh Ewald (PME) method (Beutler et al., 1994) was used to treat long range electrostatic interactions, beyond the cut-off distance of 1.0 nm. A time step of 2 fs was chosen for integration of the equations of motions. Each simulation was carried out for 200 ns. PYMOL program (Schrodinger, 2010) was used for visualizations of structures.

Curcumin was parameterized with the general AMBER force field (Wang et al, 2004) and AM1-BCC Charges (Jakalian et al, 2002) using AmberTools12 (Wang et al, 2006). GROMACS topology file of curcumin were generated from the Acpype tool (da

Silva and Vranken, 2012) and provided as appendix material. Autodock vina (Trott and Olson, 2010) was used for docking simulations of curcumin.

We have used a naming convention for our simulations; *Hp*MTAN-WT means unligated structure, *Hp*MTAN-A and *Hp*MTAN-B represents the ligation state of chain A and chain B, respectively. *Hp*MTAN-AB is used for the ligation state of the two chains.

4. RESULTS AND DISCUSSION

4.1. Docking Results

In the crystal structure, *Hp*MTAN is bounded by ligand 2-(2-hydroxyethoxy) ethylthiomethyl-DADMe-Immucillin-A. Ligand structure used for docking was obtained from CREDO database (Schreyer and Blundell, 2013). Firstly, we compared the docked ligand with the crystal structure ligand and found that the RMSD of the ligand bound to chain A and chain B of *Hp*MTAN was 0.50 Å and 1.54 Å, respectively. A ligand pose at ≤2 Å heavy-atom RMSD with respect to the crystallographic pose is acceptable (Cole et al., 2005). The same docking procedure was carried out for curcumin obtained from Pubchem (Kim et al., 2016). The best docking score of curcumin bound to both chain A and chain B of *Hp*MTAN was -8.3 kcal/mol and -7.5 kcal/mol, respectively.

4.2. RMSD Analysis

To check whether or not curcumin stays in the binding pocket of the protein during simulation, the all-atom RMSD of each curcumin with respect to a reference structure was calculated and plotted (Figure 4.1). The results show that RMSDs level off at a value between 0.1 nm and 0.8 nm approximately; suggesting that curcumin in all the complexes doesn't leave the binding site. The reason of the difference between ligand RMDSs of each complex are due to assigning random/different velocities to atoms for each trajectory. Moreover, even though curcumin bound to chain B of *Hp*MTAN in the Trajectory 3 undergoes a different conformation after 150 ns (Figure 4.1 C), it doesn't exhibit conformational changes for the rest of the complexes.

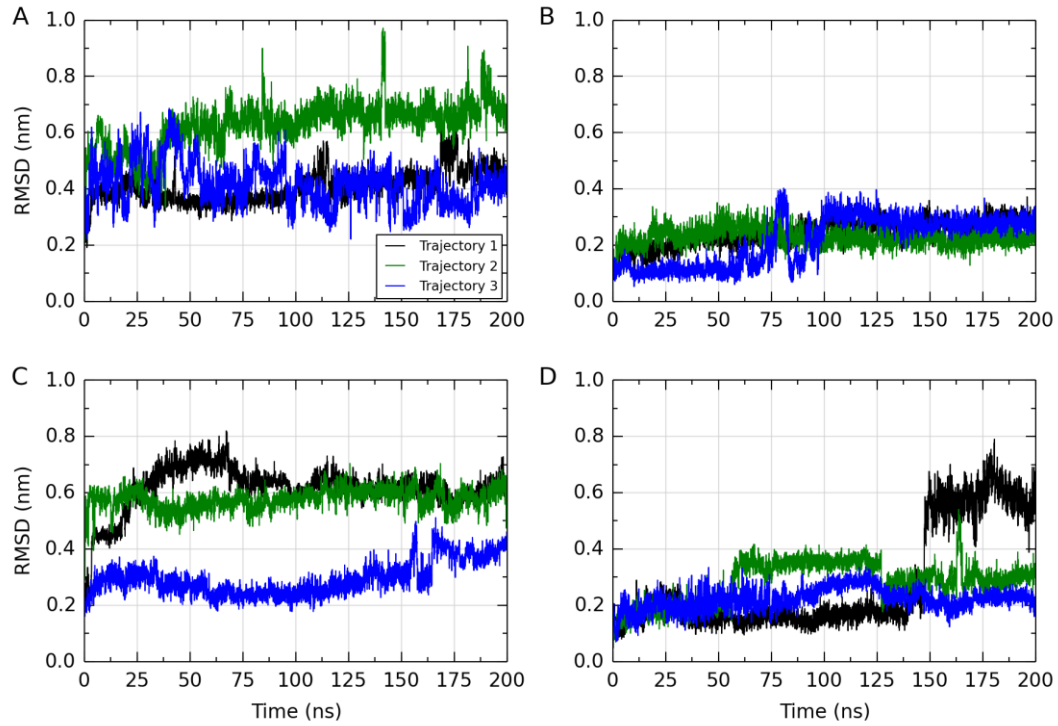

Figure 4.1. RMSDs for all trajectories of curcumin bound to (a) chain A of *Hp*MTAN-A complex, (b) chain B of *Hp*MTAN-B complex, c) chain A of *Hp*MTAN-AB complex and (d) chain B of *Hp*MTAN-AB complex. Black, green and blue colors are shown Trajectory 1, Trajectory 2 and Trajectory 3, respectively.

To investigate the structural stability of *Hp*MTAN complexes and wildtype *Hp*MTAN, Cα atom RMSD of each structure with respect to wildtype *Hp*MTAN was plotted (Figure 4.2). Overall RMSDs of all the structures level off and remain stable at ~ 0.2 nm after 100 ns. The RMSD changes of unbound *Hp*MTAN (Figure 4.2 A) and bound *Hp*MTAN complexes (Figure 4.2 B-D) are very similar to each other and are not tremendous. This indicates that curcumin does not cause important conformational changes on *Hp*MTAN. However, it should be noted that the longer simulation time such as microsecond may be needed to observe curcumin-induced conformational changes on *Hp*MTAN, if they exist.

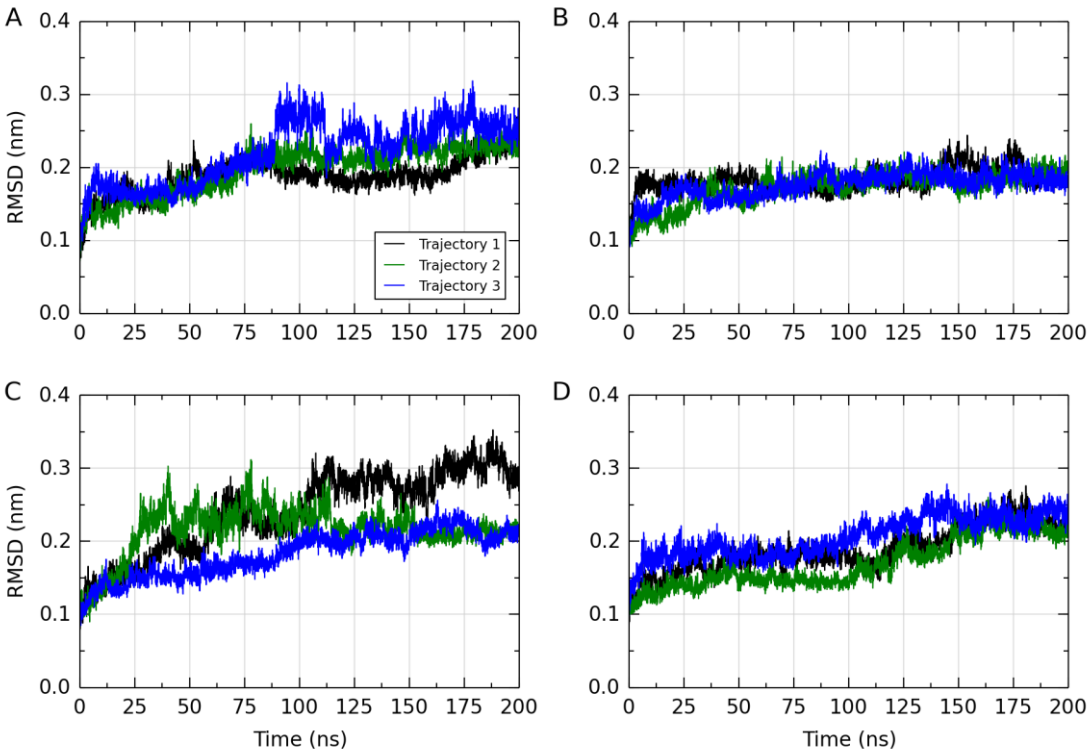

Figure 4.2. Overall RMSDs for all trajectories of (a) *Hp*MTAN-WT, (b) *Hp*MTAN-A complex, c) *Hp*MTAN-B complex and (d) *Hp*MTAN-AB complex. Black, green and blue colors are shown Trajectory 1, Trajectory 2 and Trajectory 3, respectively.

4.3. The Number of Hydrogen Bonds

We performed Hydrogen bond analysis to calculate the number of Hydrogen bonds formed between the curcumin and *Hp*MTAN (Figure 4.3). Curcumin forms Hydrogen bonds with ASP198, GLU173, VAL154, ILE52 and ALA200. The mean of Hydrogen bonds are ~ 2 between *Hp*MTAN and curcumin while curcumin is bound to chain A of *Hp*MTAN-A complex (Figure 4.3 A). Whereas, it is ~ 1 in the case of *Hp*MTAN-B complex (Figure 4.3 B). A similar result was obtained for *Hp*MTAN-AB complex as well. Curcumin forms a different number of hydrogen bonds with each chain even if it is bound to both of them (Figure 4.3 C-D). It may be a result of different docking poses (conformation) of curcumin used for both chains of *Hp*MTAN.

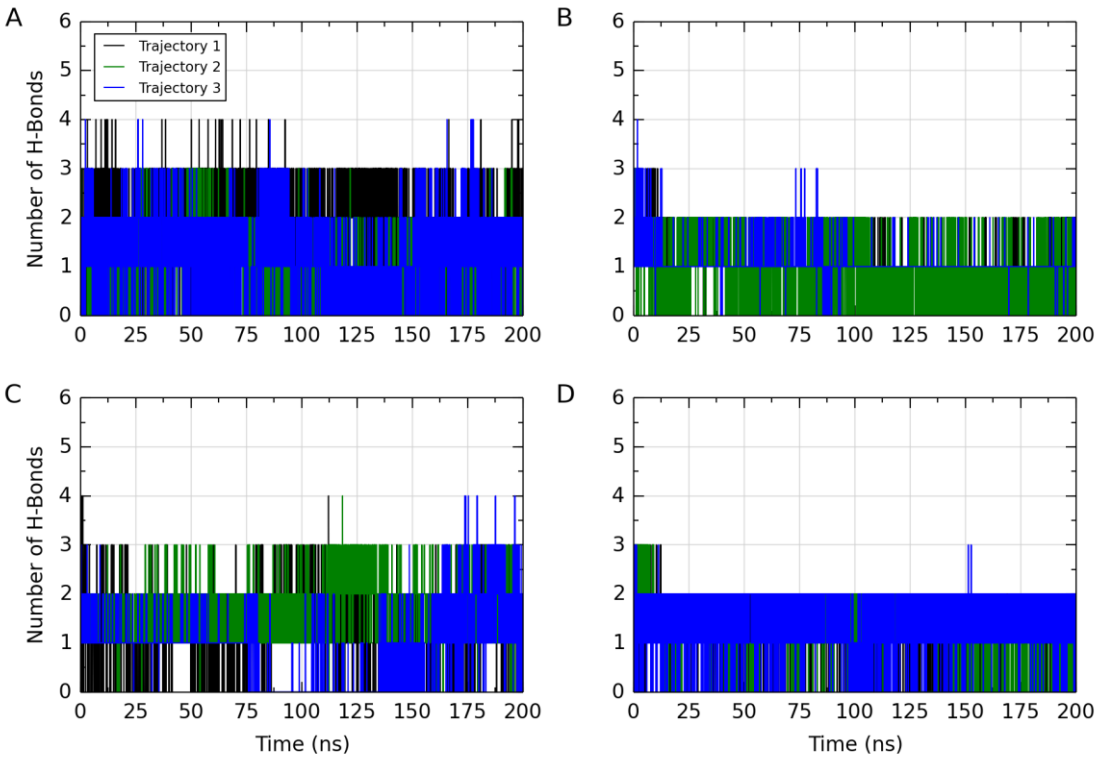

Figure 4.3. The number of Hydrogen bonds formed between (a) *Hp*MTAN and curcumin bound to chain A of *Hp*MTAN-A complex, (b) *Hp*MTAN and curcumin bound to chain B of *Hp*MTAN-B complex, c) *Hp*MTAN and curcumin bound to chain A of *Hp*MTAN-AB complex and (d) *Hp*MTAN and curcumin bound to chain B of *Hp*MTAN-AB complex. Black, green and blue colors are shown Trajectory 1, Trajectory 2 and Trajectory 3, respectively.

4.4. RMSF Analysis

Flexibility of residues contributing to protein structural fluctuations can be assessed by RMSF. As shown in Figure 4.4, the RMSF plots of all the structures in four systems indicate similar distributions, suggesting that curcumin does not lead to high structural fluctuations. Helix-6 (residues 203-228) region in all the structures shows high fluctuations of greater than 0.2 nm. Moreover, the loop consisting of residues 100-124 exhibits high fluctuations but those fluctuations are not as high as helix-6. The RMSF results imply that the fluctuations in helix-6 and loop region are related to the native behavior of the protein.

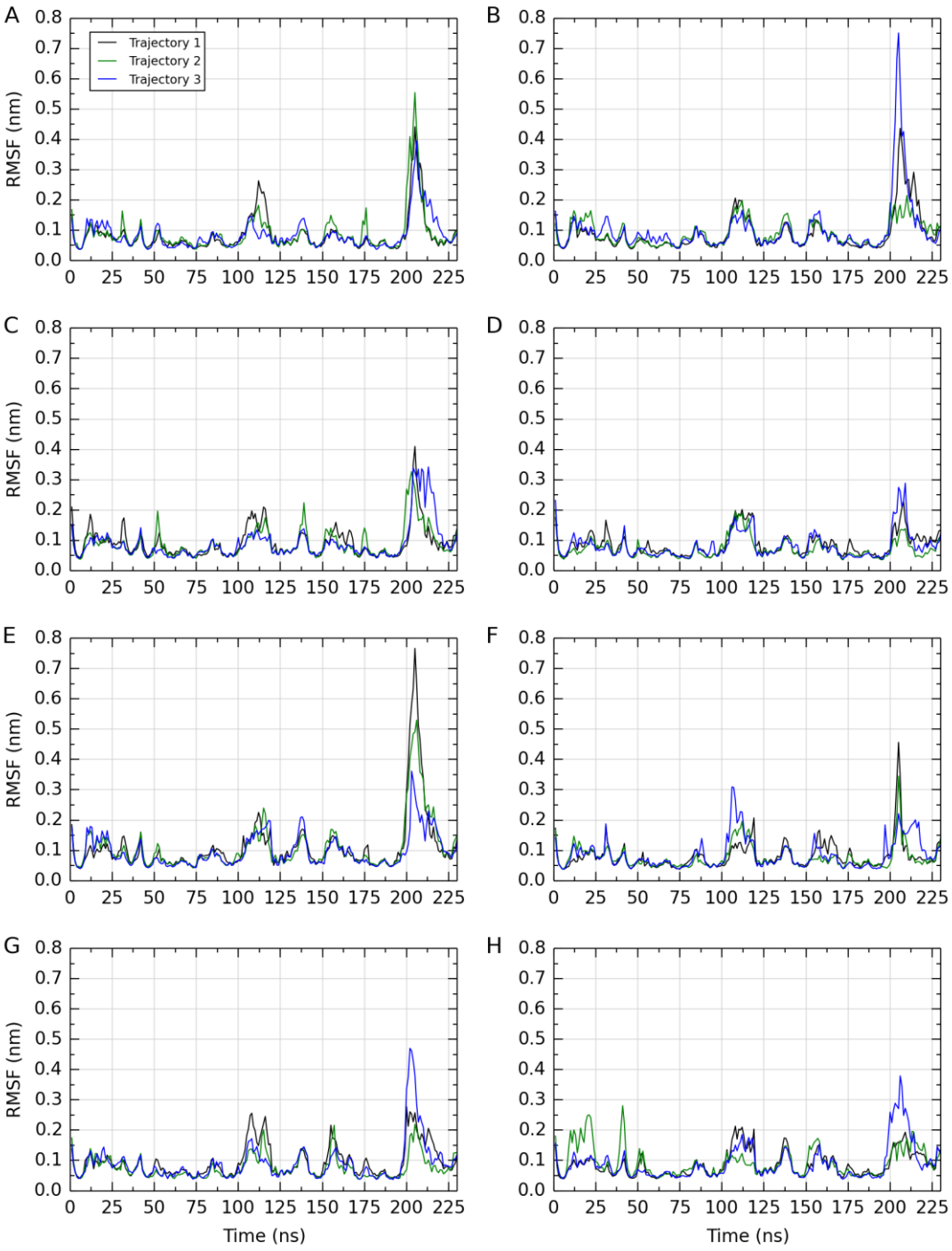

Figure 4.4. Cα atom RMSFs for all trajectories of (a-b) *Hp*MTAN-WT, (c-d) *Hp*MTAN-A complex, (e-f) *Hp*MTAN-B complex and (g-h) *Hp*MTAN-AB complex. Left and right panel represents chain A and chain B of the structures, respectively. Black, green and blue colors are shown Trajectory 1, Trajectory 2 and Trajectory 3, respectively.

4.5. Secondary Structure Analysis

Ligand bound to protein may lead to structural changes during simulation time. Changes of α-helices and/or β-sheets structures affect intramolecular and intermolecular interactions of protein. Therefore, it is important to determine the secondary structural changes of the protein during simulation time.

We plotted the secondary structure changes of all the structures studied (Figure 4.5). The results show that the most important secondary structures such as α-helices and β-sheets are conserved during simulation time, implying that curcumin does not cause any structural transitions such as from coil to helix and vice versa between secondary structures.

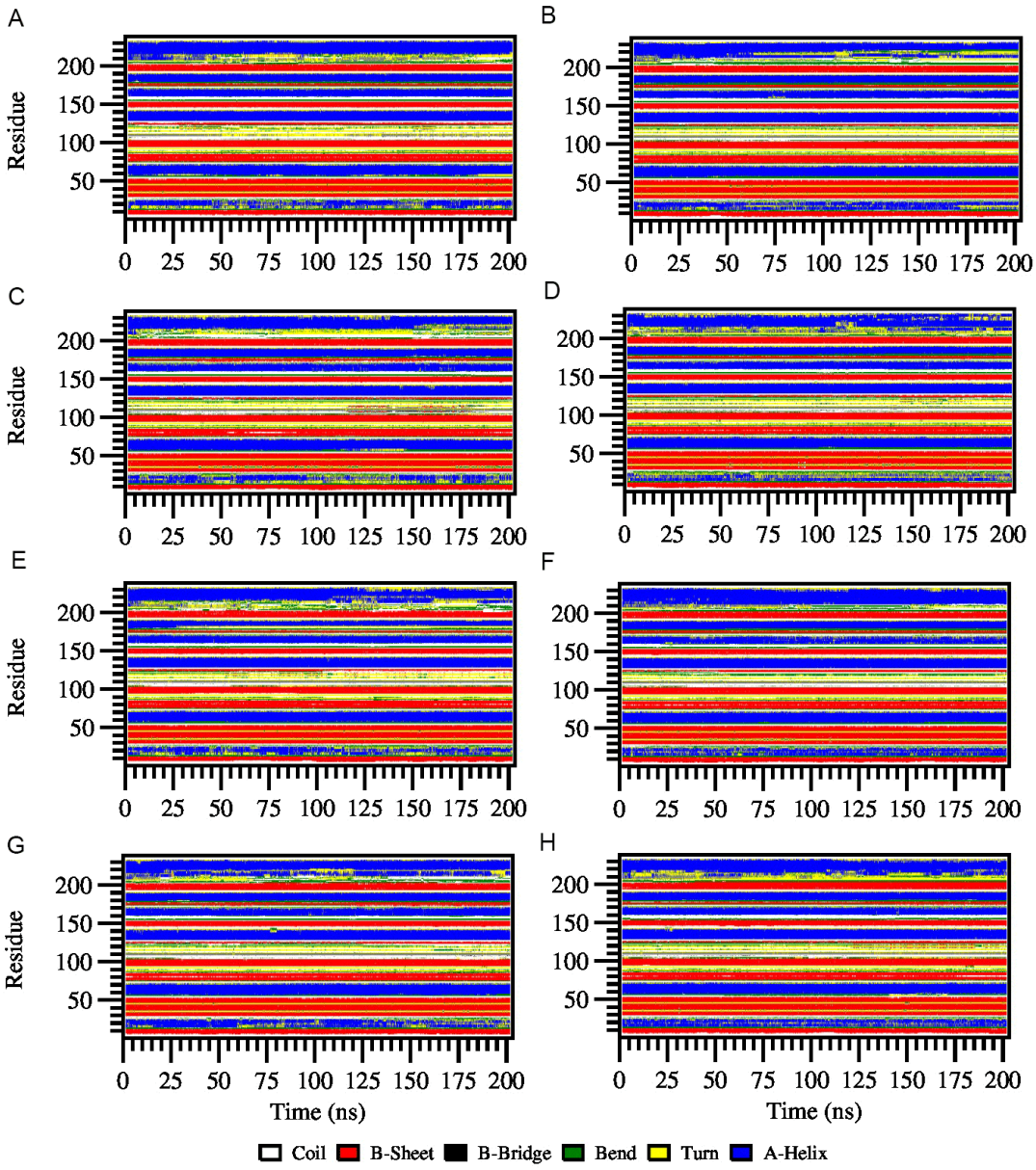

Figure 4.5. Secondary structure of (a-b) *Hp*MTAN-WT, (c-d) *Hp*MTAN-A complex, (e-f) *Hp*MTAN-B complex and (g-h) *Hp*MTAN-AB complex. Left and right panel represents chain A and chain B of the structures, respectively.

4.6. Comparison of Dynamical Cross Correlations

The dynamical cross-correlation map (DCCM) is a widely used technique to detect correlations between protein residues. DCMMs of the C-alpha atom displacement indicate correlated and anti-correlated motions in the wild type structure and in all the complexes systems as shown in Figure 4.6. The results show that DCCMs of complex structures are similar to that of wildtype structure. DCMMs of all of the structures indicate complex and anti-correlated motions as well as correlated motions. From

DCMMs results, it is not clear whether or not any groups of residues are involved in correlated and anti-correlated motions due to curcumin binding. This may be due to linear nature of DCCM.

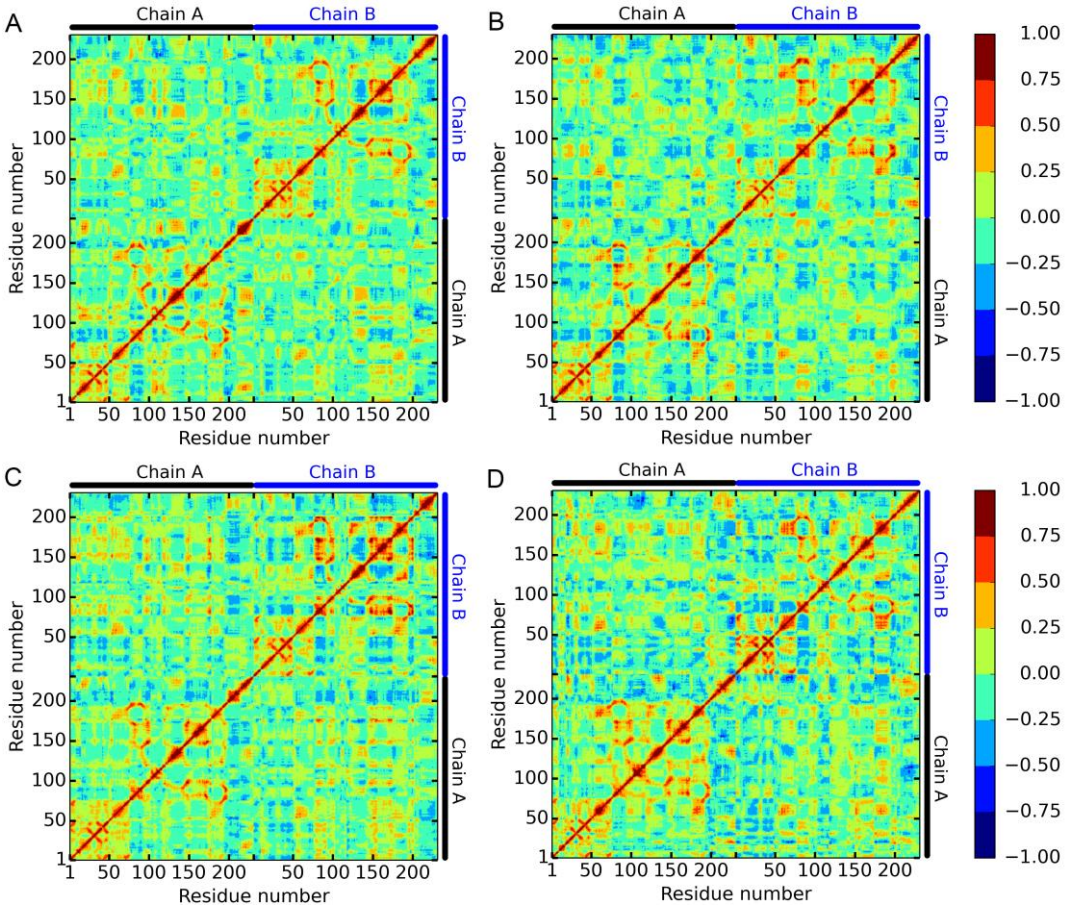

Figure 4.6. Dynamical cross-correlation map obtained from concatenated trajectories for (a) *Hp*MTAN-WT, (b) *Hp*MTAN-A complex, (c) *Hp*MTAN-B complex and (d) *Hp*MTAN-AB complex. A negative value indicates an anticorrelation between residue fluctuations whereas a positive value indicates concerted motion in the same direction (red color).

4.7. Linear Mutual Information Results

Linear Mutual Information (LMI) is another important technique to study protein dynamics. As seen in Figure 4.7, there are some local correlations when curcumin binds to each chain of *Hp*MTAN separately. Those local correlations between residues 100-230 are very obvious in case of curcumin bound to chain B of *Hp*MTAN (Figure 4.7 C). However, general correlations arise when curcumin is bound to both chains of *Hp*MTAN (Fig 4.7 D). Moreover, LMI maps show that there is no correlation between residues 125-150 of both chains of *Hp*MTAN (Fig 4.7 D). As a result, LMI plots show

that curcumin may cause intra-domain and inter-domain allosteric interactions in *Hp*MTAN.

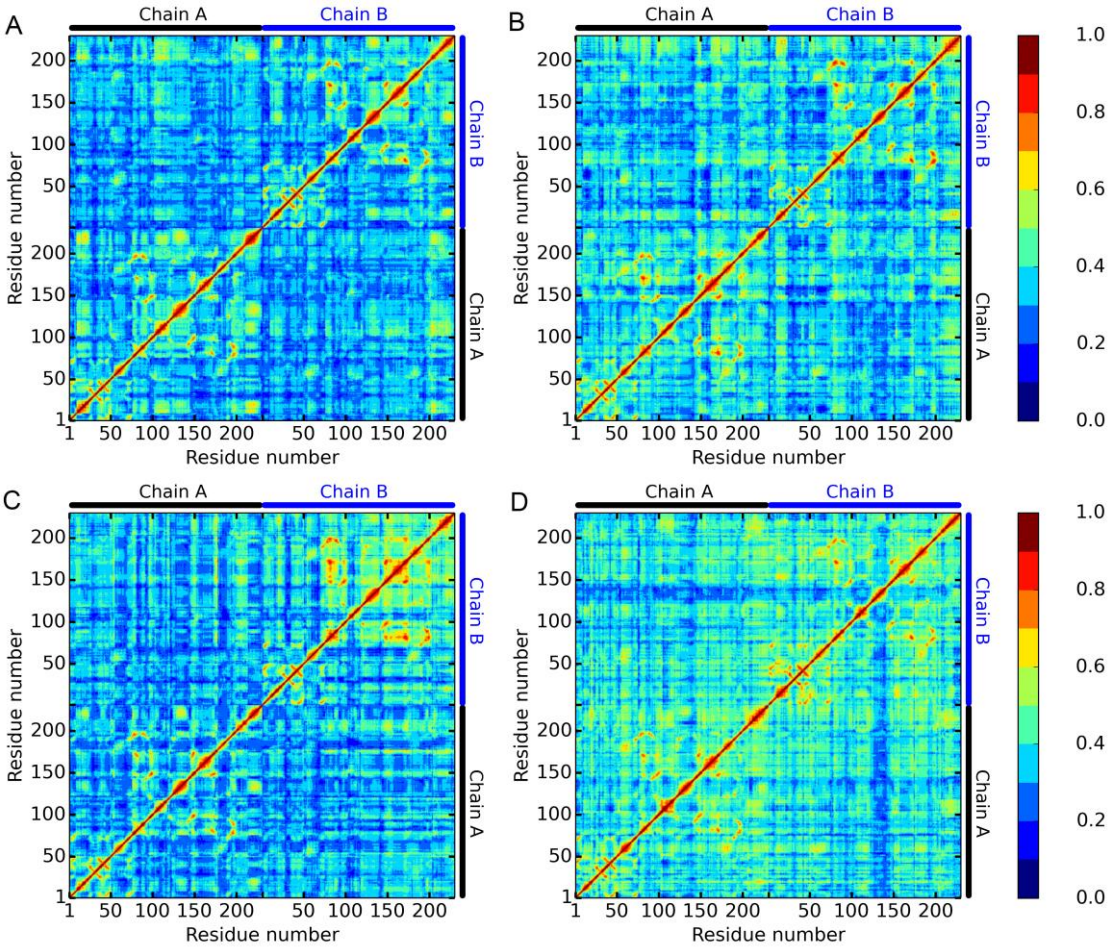

Figure 4.7. LMI metric obtained from concatenated trajectories for (a) HpMTAN-WT, (b) *Hp*MTAN-A complex, (c) *Hp*MTAN-B complex and (d) *Hp*MTAN-AB complex. 1 means correlated motions (red) and 0 means no correlation between residue fluctuations (blue).

4.8. Comparison of Generalized Correlations

Generalized correlation map (GCM) includes all the correlations, namely linear and nonlinear, in a structure. Therefore, it is a very useful method to investigate protein dynamics with this method as well. As shown in Figure 4.8, general correlations in all of the complexes have increased for both chains of *Hp*MTAN. However, non-correlated motions appear between residues 125-150 of both chains of *Hp*MTAN. This result is consistent with LMI results. The highest inter chain correlations are between residues of helix-6 (residues 203-228) in both chains. In addition, the highest intra chain

correlations are observed for helix-6 and residues 100-124 in both chains compared to wildtype *Hp*MTAN as seen in Figure 4.8 D.

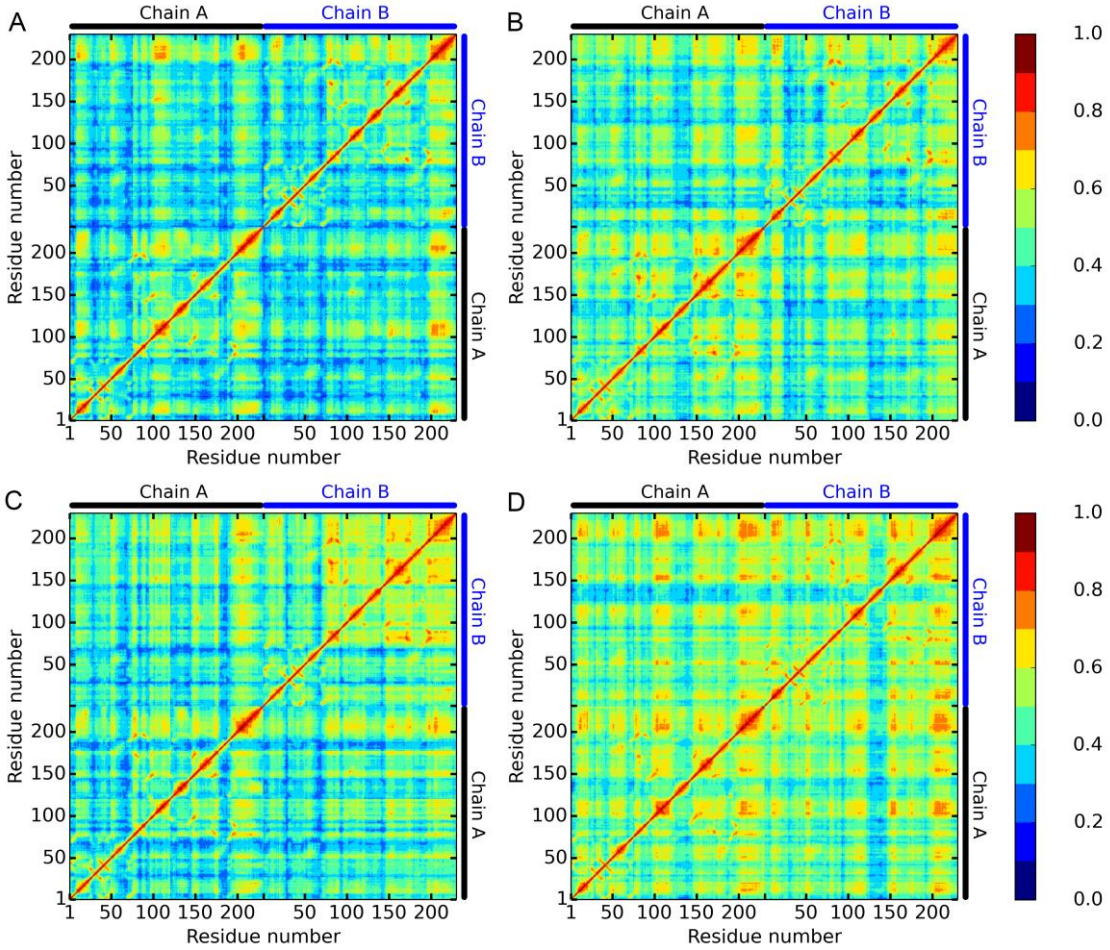

Figure 4.8. Generalized correlation map obtained from concatenated trajectories for (a) *Hp*MTAN-WT, (b) *Hp*MTAN-A complex, (c) *Hp*MTAN-B complex and (d) *Hp*MTAN-AB complex. 1 means correlated motions (red) whereas 0 means no correlation between residue fluctuations (blue).

5. CONCLUSIONS

We investigated the effect of curcumin on the conformational structure and dynamics of *Hp*MTAN using MD simulations. Our docking results reveal that curcumin has an energy of about -8 kcal/mol with *Hp*MTAN and it forms Hydrogen bonds with the active site residues ASP198, GLU173, VAL154, ILE52 and ALA200, indicating that curcumin forms strong interactions with HpMTAN, and thus can inhibit the growth of *H. pylori* infection (Vetvicka et al., 2016). In addition, it was observed that curcumin binding to *Hp*MTAN does not cause large conformational changes and large residue fluctuations.

We evaluated both inter and intra chain correlations of the wildtype *Hp*MTAN structure and *Hp*MTAN-curcumin complex systems. We found that curcumin leads to positive intra chain correlations for both helix-6 and the residues 100-124 subunits of *Hp*MTAN. The results show that while curcumin is bound to only one chain (*Hp*MTAN-A or *Hp*MTAN-B), it induces only local intra chain correlations. Whereas, in the case of curcumin bound to both chain (*Hp*MTAN-AB), it leads to general correlations, namely inter and intra chain correlations and high inter chain correlations between helix-6 motifs of both chains, suggesting that these correlations may be allosteric interactions due to curcumin binding.

On the basis of the results, we concluded that our study can provide insights into the dynamics and function of *Hp*MTAN and useful pathway information for future studies of *Hp*MTAN-curcumin complex. It also can help to understand the effect of curcumin on *H. pylori* eradication and reduction of gastric inflammation.

REFERENCES

Anonymous 2018a. https://courses.lumenlearning.com/wm-biology1/chapter/reading-amino-acids/. Access Date: 31 August 2018

Anonymous 2018b. https://courses.lumenlearning.com/microbiology/chapter/proteins/. Access Date: 31 August 2018

Anonymous 2018c. https://www.amherst.edu/system/files/media/1353/protein%252520interactions%252520F11.pdf. Access Date: 31 August 2018

Anonymous 2018d. https://bio.libretexts.org/TextMaps/Biochemistry/Book%3A_Biochemistry_Online_(Jakubowski)/01%3A_LIPID_STRUCTURE/1.3%3A_Dynamics_of_Membrane_Lipids/Molecular_Mechanics_and_Dynamics/E._Non-Bonded_Interaction_Energy. Access Date: 31 August 2018

Balachandran, P. and Govindarajan, R., 2005. Cancer-an ayurvedic perspective, *Pharmacological Research*, 51(1), 19-30.

Baron, R., Setny, P., McCammon, J.A., 2010. Water in cavity-ligand recognition, *Journal of the American Chemical Society*, 132(34), 12091-12097.

Bengmark, S., Mesa, M.D., Gil, A., 2009. Plant-derived health-the effects of turmeric and curcuminoids, *Nutricion Hospitalaria*, 24(3), 273-281.

Berendsen, H.J., Postma, J.V., van Gunsteren, W.F., DiNola, A.R.H.J., Haak, J.R., 1984. Molecular dynamics with coupling to an external bath, *The Journal of Chemical Physics*, 81(8), 3684-3690.

Beutler, T.C., Mark, A.E., van Schaik, R.C., Gerber, P.R., Van Gunsteren, W.F., 1994. Avoiding singularities and numerical instabilities in free energy calculations based on molecular simulations. *Chemical Physics Letters*, 222(6), 529-539.

Bodger, K. and Crabtree, J.E., 1998. Helicobacter pylori and gastric inflammation, *British Medical Bulletin*, 54(1), 139-150.

Bromberg, S. and Dill, K.A., 1994. Side-chain entropy and packing in proteins, *Protein Science*, 3(7), 997-1009.

Bussi, G., Donadio, D., Parrinello, M., 2007. Canonical sampling through velocity rescaling, *The Journal of Chemical Physics*, 126(1), 014101.

Chan, M.M.Y., 1995. Inhibition of tumor necrosis factor by curcumin, a phytochemical, *Biochemical Pharmacology*, 49(11), 1551-1556.

Cole, J.C., Murray, C.W., Nissink, J.W.M., Taylor, R.D., Taylor, R., 2005. Comparing protein–ligand docking programs is difficult, *Proteins: Structure, Function, and Bioinformatics*, 60(3), 325-332.

Cornell, W.D., Cieplak, P., Bayly, C.I., Gould, I.R., Merz, K.M., Ferguson, D.M., Spellmeyer, D.C., Fox, T., Caldwell, J.W., Kollman, P.A., 1995. A second generation force field for the simulation of proteins, nucleic acids, and organic molecules, *Journal of the American Chemical Society*, 117(19), 5179-5197.

Correa, P., Cuello, C., Duque, E., Burbano, L.C., Garcia, F.T., Bolanos, O., Brown, C., Haenszel, W., 1976. Gastric cancer in Colombia. III. Natural history of precursor lesions, *Journal of the National Cancer Institute*, 57(5), 1027-1035.

da Silva, A.S. and Vranken, W., 2012. ACPYPE-AnteChamber Python Parser interfacE. *BMC Res Notes* 5:1-8.

De Falco, M., Lucariello, A., Iaquinto, S., Esposito, V., Guerra, G., De Luca, A., 2015. Molecular mechanisms of Helicobacter pylori pathogenesis, *Journal of Cellular Physiology*, 230(8), 1702-1707.

Di Mario, F., Cavallaro, L.G., Nouvenne, A., Stefani, N., Cavestro, G.M., Iori, V., Maino, M., Comparato, G., Fanigliulo, L., Morana, E., Pilotto, A., 2007. A curcumin-based 1-week triple therapy for eradication of Helicobacter pylori infection: something to learn from failure? *Helicobacter*, 12(3), pp.238-243.

Dill, K.A., Bromberg, S., Yue, K., Chan, H.S., Ftebig, K.M., Yee, D.P., Thomas, P.D., 1995. Principles of protein folding-a perspective from simple exact models, *Protein Science*, 4(4), 561-602.

Dooley, C.P. and Cohen, H., 1988. The clinical significance of Campylobacter pylori, *Annals of internal medicine*, 108(1), 70-79.

Foryst-Ludwig, A., Neumann, M., Schneider-Brachert, W., Naumann, M., 2004. Curcumin blocks NF-κB and the motogenic response in Helicobacter pylori-

infected epithelial cells, *Biochemical and Biophysical Research Communications*, 316(4), 1065-1072.

Gao, X., Kuo, J., Jiang, H., Deeb, D., Liu, Y., Divine, G., Chapman, R.A., Dulchavsky, S.A., Gautam, S.C., 2004. Immunomodulatory activity of curcumin: suppression of lymphocyte proliferation, development of cell-mediated cytotoxicity, and cytokine production in vitro, *Biochemical Pharmacology*, 68(1), 51-61.

Goel, A., Kunnumakkara, A.B. and Aggarwal, B.B., 2008. Curcumin as "Curecumin": from kitchen to clinic, *Biochemical Pharmacology*, 75(4), 787-809.

Graham, D.Y., Klein, P.D., Opekun, A.R., Boutton, T.W., 1988. Effect of Age on the Frequency of Active Campylobacter pylori Infection Diagnosed by the [13] Urea Breath Test in Normal Subjects and Patients with Peptic Ulcer Disease, *Journal of Infectious Diseases*, 157(4), 777-780.

Grant, B.J., Rodrigues, A.P., ElSawy, K.M., McCammon, J.A., Caves, L.S., 2006. Bio3d: an R package for the comparative analysis of protein structures, *Bioinformatics*, 22(21), 2695-2696.

Gutierrez, J.A., Crowder, T., Rinaldo-Matthis, A., Ho, M.C., Almo, S.C. and Schramm, V.L., 2009. Transition state analogs of 5′-methylthioadenosine nucleosidase disrupt quorum sensing, *Nature Chemical Biology*, 5(4), 251.

Gutierrez, J.A., Luo, M., Singh, V., Li, L., Brown, R.L., Norris, G.E., Evans, G.B., Furneaux, R.H., Tyler, P.C., Painter, G.F., Lenz, D.H., 2007. Picomolar inhibitors as transition-state probes of 5′-methylthioadenosine nucleosidases, *ACS Chemical Biology*, 2(11), 725-734.

Hess, B., Bekker, H., Berendsen, H.J., Fraaije, J.G., 1997. LINCS: a linear constraint solver for molecular simulations, *Journal of Computational Chemistry*, 18(12), 1463-1472.

Hiratsuka, T., Furihata, K., Ishikawa, J., Yamashita, H., Itoh, N., Seto, H., Dairi, T., 2008. An alternative menaquinone biosynthetic pathway operating in microorganisms, *Science*, 321(5896), 1670-1673.

Hospital, A., Goñi, J.R., Orozco, M., Gelpí, J.L., 2015. Molecular dynamics simulations: advances and applications, *Advances and Applications in Bioinformatics and Chemistry: AABC*, 8, 37.

Ihamäki, T., Varis, K., Siurala, M., 1979. Morphological, functional and immunological state of the gastric mucosa in gastric carcinoma families: comparison with a computer-matched family sample, *Scandinavian Journal of Gastroenterology*, 14(7), 801-812.

J.W. Suttie, 2009. Vitamin K in Health and Disease; New York, *CRC Press*.

Jakalian, A., Jack, D.B., Bayly, C.I., 2002. Fast, efficient generation of high-quality atomic charges. AM1-BCC model: II. Parameterization and validation, *Journal of Computational Chemistry*, 23(16), 1623-1641.

Jones, D.M., Eldridge, J., Fox, A.J., Sethi, P., Whorwell, P.J., 1986. Antibody to the gastric campylobacter-like organism ("Campylobacter pyloridis")—clinical correlations and distribution in the normal population, *Journal of Medical Microbiology*, 22(1), 57-62.

Jones, J.E., 1924. On the determination of molecular fields, II. From the equation of state of a gas, *Proc. R. Soc. Lond. A*, 106(738), 463-477.

Jorgensen, W.L., Chandrasekhar, J., Madura, J.D., Impey, R.W., Klein, M.L., 1983. Comparison of simple potential functions for simulating liquid water, *The Journal of Chemical Physics*, 79(2), 926-935.

Jorgensen, W.L., Maxwell, D.S., Tirado-Rives, J., 1996. Development and testing of the OPLS all-atom force field on conformational energetics and properties of organic liquids, *Journal of the American Chemical Society*, 118(45), 11225-11236.

Kaldor, J., Tee, W., Nicolacopolous, C., Demirtzoglou, K., Noonan, D., Dwyer, B., 1986. Immunoblot confirmation of immune response to Campylobacter pyloridis in patients with duodenal ulcers, *The Medical Journal of Australia*, 145(3-4), 133-135.

Kewitz, S., Volkmer, I., Staege, M.S., 2013. Curcuma contra cancer? Curcumin and Hodgkin's lymphoma, *Cancer Growth and Metastasis*, 6, 35-52.

Kim, A., Lim, J.W., Kim, H, Kim, H., 2016. Supplementation with Angelica keiskei inhibits expression of inflammatory mediators in the gastric mucosa of Helicobacter pylori-infected mice, *Nutrition Research*, 36(5), 488-497.

Kim, S., Thiessen, P.A., Bolton, E.E., Chen, J., Fu, G., Gindulyte, A., Han, L., He, J., He, S., Shoemaker, B.A., Wang, J., 2015. PubChem substance and compound databases, *Nucleic Acids Research*, 44, 1202-1213.

Kouza, M., 2013. Numerical Simulation of Folding and Unfolding of Proteins, *arXiv* 1308, 2380.

Kuipers, E.J., Thijs, J.C., Festen, H.P., 1995. The prevalence of Helicobacter pylori in peptic ulcer disease, *Alimentary Pharmacology & Therapeutics*, 9, 59-69.

Kundu, P., De, R., Pal, I., Mukhopadhyay, A.K., Saha, D.R., Swarnakar, S., 2011. Curcumin alleviates matrix metalloproteinase-3 and-9 activities during eradication of Helicobacter pylori infection in cultured cells and mice, *PloS one*, 6(1), 16306.

Kurosu, M. and Begari, E., 2010. Vitamin K2 in electron transport system: are enzymes involved in vitamin K2 biosynthesis promising drug targets? *Molecules*, 15(3), 1531-1553.

Lange, O.F. and Grubmüller, H., 2006. Generalized correlation for biomolecular dynamics, *Proteins: Structure, Function, and Bioinformatics*, 62(4), 1053-1061.

Li, X., Apel, D., Gaynor, E.C., Tanner, M.E., 2011. 5'-methylthioadenosine nucleosidase is implicated in playing a key role in a modified futalosine pathway for menaquinone biosynthesis in Campylobacter jejuni, *Journal of Biological Chemistry*, *286*, 19392.

Lindahl, E., Hess, B., Van Der Spoel, D., 2001. GROMACS 3.0: a package for molecular simulation and trajectory analysis, *Molecular Modeling Annual*, 7(8), 306-317.

Lindorff-Larsen, K., Piana, S., Palmo, K., Maragakis, P., Klepeis, J.L., Dror, R.O., Shaw, D.E., 2010. Improved side-chain torsion potentials for the Amber ff99SB protein force field, *Proteins: Structure, Function, and Bioinformatics*, *78*(8), 1950-1958.

MacKerell, A.D., Brooks, C.L., Nilsson, L., Roux, B., Won, Y., Karplus, M., 1998. CHARMM: The energy function and its parameterization with an overview of the program, *John Wiley & Sons*, 271-277.

Maroon, J.C., Bost, J.W., Maroon, A., 2010. Natural anti-inflammatory agents for pain relief, *Surgical Neurology International*, 1, 80.

Marshall, B., Warren, J.R., Blincow, E., Phillips, M., Goodwin, C.S., Murray, R., Blackbourn, S., Waters, T., Sanderson, C., 1988. Prospective double-blind trial of duodenal ulcer relapse after eradication of Campylobacter pylori, *The Lancet*, 332(8626-8627), 1437-1442.

McNulty, C.A., Dent, J., Wise, R., 1985. Susceptibility of clinical isolates of Campylobacter pyloridis to 11 antimicrobial agents, *Antimicrobial Agents and Chemotherapy*, 28(6), 837-838.

McNulty, C.A., Gearty, J.C., Crump, B., Davis, M., Donovan, I.A., Melikian, V., Lister, D.M., Wise, R., 1986. Campylobacter pyloridis and associated gastritis: investigator blind, placebo controlled trial of bismuth salicylate and erythromycin ethylsuccinate, *Br. Med. J.*, 293(6548), 645-649.

Miller, C.H. and Duerre, J.A., 1968. S-ribosylhomocysteine cleavage enzyme from Escherichia coli, *Journal of Biological Chemistry*, 243(1), 92-97.

Miller, M.B. and Bassler, B.L., 2001. Quorum sensing in bacteria, *Annual Reviews in Microbiology*, 55(1), 165-199.

Mishra, V. and Ronning, D.R., 2012. Crystal structures of the Helicobacter pylori MTAN enzyme reveal specific interactions between S-adenosylhomocysteine and the 5′-alkylthio binding subsite, *Biochemistry*, 51(48), 9763-9772.

Moon, D.O., Jin, C.Y., Lee, J.D., Choi, Y.H., Ahn, S.C., Lee, C.M., Jeong, S.C., Park, Y.M., Kim, G.Y., 2006. Curcumin Decreases Binding of Shiga-Like Toxin-1B on Human Intestinal Epithelial Cell Line HT29 Stimulated with TNF-α and IL-1β: Suppression of p38, JNK and NF-κB p65 as Potential Targets, *Biological and Pharmaceutical Bulletin*, 29(7), 1470-1475.

Oostenbrink, C., Villa, A., Mark, A.E., Van Gunsteren, W.F., 2004. A biomolecular force field based on the free enthalpy of hydration and solvation: the GROMOS force-field parameter sets 53A5 and 53A6, *Journal of Computational Chemistry*, 25(13), 1656-1676.

Parrinello, M. and Rahman, A., 1981. Polymorphic transitions in single crystals: A new molecular dynamics method, *Journal of Applied physics*, 52(12), 7182-7190.

Parveen, N. and Cornell, K.A., 2011. Methylthioadenosine/S-adenosylhomocysteine nucleosidase, a critical enzyme for bacterial metabolism, *Molecular Microbiology*, 79(1), 7-20.

Paull, G. and Yardley, J.H., 1988. Gastric and esophageal Campylobacter pylori in patients with Barrett's esophagus, *Gastroenterology*, 95(1), 216-218.

Popp, J.L., Berliner, C., Bentley, R., 1989. Vitamin K (menaquinone) biosynthesis in bacteria: high-performance liquid chromatographic assay of the overall synthesis of o-succinylbenzoic acid and of 2-succinyl-6-hydroxy-2, 4-cyclohexadiene-1-carboxylic acid synthase, *Analytical Biochemistry*, 178(2), 306-310.

Rad, R., Brenner, L., Krug, A., Voland, P., Mages, J., Lang, R., Schwendy, S., Reindl, W., Dossumbekova, A., Ballhorn, W., Wagner, H., 2007. Toll-like receptor–dependent activation of antigen-presenting cells affects adaptive immunity to Helicobacter pylori, *Gastroenterology*, 133(1), 150-163.

Richardson, J.S., 1981. The anatomy and taxonomy of protein structure, *In Advances in Protein Chemistry*, 34, 167-339.

Ruby, A.J., Kuttan, G., Babu, K.D., Rajasekharan, K.N., Kuttan, R., 1995. Anti-tumour and antioxidant activity of natural curcuminoids, *Cancer Letters*, 94(1), 79-83.

Santos, A.M., Lopes, T., Oleastro, M., Gato, I.V., Floch, P., Benejat, L., Chaves, P., Pereira, T., Seixas, E., Machado, J., Guerreiro, A.S., 2015. Curcumin inhibits gastric inflammation induced by Helicobacter pylori infection in a mouse model, *Nutrients*, 7(1), 306-320.

Sarkar, A., De, R., Mukhopadhyay, A.K., 2016. Curcumin as a potential therapeutic candidate for Helicobacter pylori associated diseases, *World Journal of Gastroenterology*, 22(9), 2736.

Schramm, V.L., 2005. Enzymatic transition states: thermodynamics, dynamics and analogue design. *Archives of Biochemistry and Biophysics*, 433(1), 13-26.

Schreyer, A.M. and Blundell, T.L., 2013. CREDO: a structural interactomics database for drug discovery, Database.

Schrodinger, LLC., 2010. The PyMOL Molecular Graphics System, Version 1.3r1.

Selgrad, M. and Malfertheiner, P., 2011. Treatment of Helicobacter pylori, *Current Opinion in Gastroenterology*, 27(6), 565-570.

Seto, H., Jinnai, Y., Hiratsuka, T., Fukawa, M., Furihata, K., Itoh, N., Dairi, T., 2008. Studies on a new biosynthetic pathway for menaquinone, *Journal of the American Chemical Society*, 130(17), 5614-5615.

Sintara, K., Thong-Ngam, D., Patumraj, S., Klaikeaw, N., Chatsuwan, T., 2010. Curcumin suppresses gastric NF-κB activation and macromolecular leakage in Helicobacter pylori-infected rats, *World Journal of Gastroenterology: WJG*, 16(32), 4039.

Siurala, M., Isokoski, M., Varis, K., Kekki, M., 1968. Prevalence of gastritis in a rural population: bioptic study of subjects selected at random, *Scandinavian Journal of Gastroenterology*, 3(2), 211-223.

Surh, Y.J., 2002. Anti-tumor promoting potential of selected spice ingredients with antioxidative and anti-inflammatory activities: a short review, *Food and Chemical Toxicology*, 40(8), 1091-1097.

Teif, V.B. and Rippe, K., 2010. Statistical–mechanical lattice models for protein–DNA binding in chromatin, *Journal of Physics: Condensed Matter*, 22(41), 414105.

Teif, V.B., 2005. Ligand-induced DNA condensation: choosing the model, *Biophysical journal*, 89(4), 2574-2587.

Tekpinar, M., Yildirim, A., Wassenaar, T.A., 2015. Molecular dynamics study of the effect of active site protonation on Helicobacter pylori 5′-methylthioadenosine/S-adenosylhomocysteine nucleosidase, *European Biophysics Journal*, 44(8), 685-696.

Trott, O. and Olson, A.J., 2010. AutoDock Vina: improving the speed and accuracy of docking with a new scoring function, efficient optimization, and multithreading, *Journal of Computational Chemistry*, *31*(2), pp.455-461.

van Gunsteren, W.F. and Berendsen, H.J., 1990. Computer simulation of molecular dynamics: Methodology, applications, and perspectives in chemistry, *Angewandte Chemie International Edition in English*, *29*(9), 992-1023.

Verlet, L., 1967. Computer experiments on classical fluids. I. Thermodynamical properties of Lennard-Jones molecules, *Physical Review*, 159(1), 98-103.

Vetvicka, V., Vetvickova, J., Fernandez-Botran, R., 2016. Effects of curcumin on Helicobacter pylori infection, *Annals of Translational Medicine*, 4(24).

Villako, K., Tamm, A., Savisaar, E., Ruttas, M., 1976. Prevalence of antral and fundic gastritis in a randomly selected group of an Estonian rural population, *Scandinavian Journal of Gastroenterology*, 11(8), 817-822.

Wang, J., Wang, W., Kollman, P.A., Case, D.A., 2006. Automatic atom type and bond type perception in molecular mechanical calculations, *Journal of Molecular Graphics and Modelling*, *25*(2), 247-260.

Wang, J., Wolf, R.M., Caldwell, J.W., Kollman, P.A., Case, D.A., 2004. Development and testing of a general amber force field, *Journal of Computational Chemistry*, *25*(9), 1157-1174.

Wang, S., Cameron, S.A., Clinch, K., Evans, G.B., Wu, Z., Schramm, V.L., Tyler, P.C., 2015. New antibiotic candidates against helicobacter pylori, *Journal of the American Chemical Society*, *137*(45), 14275-14280.

Wang, S., Haapalainen, A.M., Yan, F., Du, Q., Tyler, P.C., Evans, G.B., Rinaldo-Matthis, A., Brown, R.L., Norris, G.E., Almo, S.C., Schramm, V.L., 2012. A picomolar transition state analogue inhibitor of MTAN as a specific antibiotic for Helicobacter pylori, *Biochemistry*, 51(35), 6892-6894.

Westbrook, J., Feng, Z., Jain, S., Bhat, T.N., Thanki, N., Ravichandran, V., Gilliland, G.L., Bluhm, W., Weissig, H., Greer, D.S., Bourne, P.E., 2002. The protein data bank: unifying the archive, *Nucleic Acids Research*, 30(1), 245-248.

Y. Wang, and J.A. McCammon, 2012. Computational Modeling of Biological Systems. Editor: Nikolay Dokholyan. Part1. Introduction to Molecular Dynamics: Theory and Applications in Biomolecular Modeling, New York Dordrecht Heidelberg, London, *Springer*.

APPENDIX

```
; curcumin.top created by acpype

[ defaults ]
; nbfunc        comb-rule       gen-pairs       fudgeLJ fudgeQQ
1               2               yes             0.5     0.8333

[ atomtypes ]
;name   bond_type     mass     charge   ptype   sigma         epsilon       Amb
 os       os          0.00000  0.00000   A     3.00001e-01   7.11280e-01 ; 1.68  0.1700
 oh       oh          0.00000  0.00000   A     3.06647e-01   8.80314e-01 ; 1.72  0.2104
 o        o           0.00000  0.00000   A     2.95992e-01   8.78640e-01 ; 1.66  0.2100
 ca       ca          0.00000  0.00000   A     3.39967e-01   3.59824e-01 ; 1.91  0.0860
 c3       c3          0.00000  0.00000   A     3.39967e-01   4.57730e-01 ; 1.91  0.1094
 ce       ce          0.00000  0.00000   A     3.39967e-01   3.59824e-01 ; 1.91  0.0860
 c        c           0.00000  0.00000   A     3.39967e-01   3.59824e-01 ; 1.91  0.0860
 cf       cf          0.00000  0.00000   A     3.39967e-01   3.59824e-01 ; 1.91  0.0860
 hc       hc          0.00000  0.00000   A     2.64953e-01   6.56888e-02 ; 1.49  0.0157
 ha       ha          0.00000  0.00000   A     2.59964e-01   6.27600e-02 ; 1.46  0.0150
 ho       ho          0.00000  0.00000   A     0.00000e+00   0.00000e+00 ; 0.00  0.0000
 h1       h1          0.00000  0.00000   A     2.47135e-01   6.56888e-02 ; 1.39  0.0157

[ moleculetype ]
;name            nrexcl
 LIG              3

[ atoms ]
;   nr  type  resi  res  atom  cgnr     charge      mass       ; qtot   bond_type
     1    os     1   LIG    O1     1   -0.325900     16.00000 ; qtot -0.326
     2    os     1   LIG    O2     2   -0.325900     16.00000 ; qtot -0.652
     3    oh     1   LIG    O3     3   -0.480100     16.00000 ; qtot -1.132
     4    oh     1   LIG    O4     4   -0.480100     16.00000 ; qtot -1.612
     5     o     1   LIG    O5     5   -0.541101     16.00000 ; qtot -2.153
     6     o     1   LIG    O6     6   -0.541101     16.00000 ; qtot -2.694
     7    ca     1   LIG    C1     7   -0.090300     12.01000 ; qtot -2.785
     8    ca     1   LIG    C2     8   -0.090300     12.01000 ; qtot -2.875
     9    c3     1   LIG    C3     9   -0.284400     12.01000 ; qtot -3.159
    10    ca     1   LIG    C4    10   -0.145500     12.01000 ; qtot -3.305
    11    ca     1   LIG    C5    11   -0.145500     12.01000 ; qtot -3.450
    12    ca     1   LIG    C6    12    0.066600     12.01000 ; qtot -3.384
    13    ca     1   LIG    C7    13    0.066600     12.01000 ; qtot -3.317
    14    ca     1   LIG    C8    14   -0.092500     12.01000 ; qtot -3.410
    15    ca     1   LIG    C9    15   -0.092500     12.01000 ; qtot -3.502
    16    ce     1   LIG   C10    16   -0.007700     12.01000 ; qtot -3.510
    17    ce     1   LIG   C11    17   -0.007700     12.01000 ; qtot -3.517
    18    ca     1   LIG   C12    18    0.126600     12.01000 ; qtot -3.391
    19    ca     1   LIG   C13    19    0.126600     12.01000 ; qtot -3.264
    20     c     1   LIG   C14    20    0.578301     12.01000 ; qtot -2.686
    21     c     1   LIG   C15    21    0.578301     12.01000 ; qtot -2.108
    22    ca     1   LIG   C16    22   -0.172000     12.01000 ; qtot -2.280
    23    ca     1   LIG   C17    23   -0.172000     12.01000 ; qtot -2.452
    24    cf     1   LIG   C18    24   -0.276200     12.01000 ; qtot -2.728
    25    cf     1   LIG   C19    25   -0.276200     12.01000 ; qtot -3.004
    26    c3     1   LIG   C20    26    0.114700     12.01000 ; qtot -2.889
    27    c3     1   LIG   C21    27    0.114700     12.01000 ; qtot -2.775
    28    hc     1   LIG    H1    28    0.090700      1.00800 ; qtot -2.684
    29    hc     1   LIG    H2    29    0.090700      1.00800 ; qtot -2.593
    30    ha     1   LIG    H3    30    0.144000      1.00800 ; qtot -2.449
    31    ha     1   LIG    H4    31    0.144000      1.00800 ; qtot -2.305
    32    ha     1   LIG    H5    32    0.143500      1.00800 ; qtot -2.162
    33    ha     1   LIG    H6    33    0.143500      1.00800 ; qtot -2.018
    34    ha     1   LIG    H7    34    0.143000      1.00800 ; qtot -1.875
    35    ha     1   LIG    H8    35    0.143000      1.00800 ; qtot -1.732
    36    ha     1   LIG    H9    36    0.149000      1.00800 ; qtot -1.583
    37    ha     1   LIG   H10    37    0.149000      1.00800 ; qtot -1.434
    38    ha     1   LIG   H11    38    0.148000      1.00800 ; qtot -1.286
    39    ha     1   LIG   H12    39    0.148000      1.00800 ; qtot -1.138
    40    ho     1   LIG   H13    40    0.429000      1.00800 ; qtot -0.709
    41    ho     1   LIG   H14    41    0.429000      1.00800 ; qtot -0.280
    42    h1     1   LIG   H15    42    0.046700      1.00800 ; qtot -0.234
    43    h1     1   LIG   H16    43    0.046700      1.00800 ; qtot -0.187
    44    h1     1   LIG   H17    44    0.046700      1.00800 ; qtot -0.140
    45    h1     1   LIG   H18    45    0.046700      1.00800 ; qtot -0.093
    46    h1     1   LIG   H19    46    0.046700      1.00800 ; qtot -0.047
    47    h1     1   LIG   H20    47    0.046700      1.00800 ; qtot 0.000
```

```
[ bonds ]
;   ai     aj funct   r             k
     1     12   1    1.3730e-01    3.1162e+05 ;     O1 - C6
     1     26   1    1.4390e-01    2.5230e+05 ;     O1 - C20
     2     13   1    1.3730e-01    3.1162e+05 ;     O2 - C7
     2     27   1    1.4390e-01    2.5230e+05 ;     O2 - C21
     3     18   1    1.3620e-01    3.2309e+05 ;     O3 - C12
     3     40   1    9.7400e-02    3.0928e+05 ;     O3 - H13
     4     19   1    1.3620e-01    3.2309e+05 ;     O4 - C13
     4     41   1    9.7400e-02    3.0928e+05 ;     O4 - H14
     5     20   1    1.2140e-01    5.4225e+05 ;     O5 - C14
     6     21   1    1.2140e-01    5.4225e+05 ;     O6 - C15
     7     10   1    1.3870e-01    4.0033e+05 ;     C1 - C4
     7     14   1    1.3870e-01    4.0033e+05 ;     C1 - C8
     7     16   1    1.4720e-01    3.0627e+05 ;     C1 - C10
     8     11   1    1.3870e-01    4.0033e+05 ;     C2 - C5
     8     15   1    1.3870e-01    4.0033e+05 ;     C2 - C9
     8     17   1    1.4720e-01    3.0627e+05 ;     C2 - C11
     9     20   1    1.5080e-01    2.7472e+05 ;     C3 - C14
     9     21   1    1.5080e-01    2.7472e+05 ;     C3 - C15
     9     28   1    1.0920e-01    2.8225e+05 ;     C3 - H1
     9     29   1    1.0920e-01    2.8225e+05 ;     C3 - H2
    10     12   1    1.3870e-01    4.0033e+05 ;     C4 - C6
    10     30   1    1.0870e-01    2.8811e+05 ;     C4 - H3
    11     13   1    1.3870e-01    4.0033e+05 ;     C5 - C7
    11     31   1    1.0870e-01    2.8811e+05 ;     C5 - H4
    12     18   1    1.3870e-01    4.0033e+05 ;     C6 - C12
    13     19   1    1.3870e-01    4.0033e+05 ;     C7 - C13
    14     22   1    1.3870e-01    4.0033e+05 ;     C8 - C16
    14     32   1    1.0870e-01    2.8811e+05 ;     C8 - H5
    15     23   1    1.3870e-01    4.0033e+05 ;     C9 - C17
    15     33   1    1.0870e-01    2.8811e+05 ;     C9 - H6
    16     24   1    1.3380e-01    4.7062e+05 ;    C10 - C18
    16     34   1    1.0890e-01    2.8577e+05 ;    C10 - H7
    17     25   1    1.3380e-01    4.7062e+05 ;    C11 - C19
    17     35   1    1.0890e-01    2.8577e+05 ;    C11 - H8
    18     22   1    1.3870e-01    4.0033e+05 ;    C12 - C16
    19     23   1    1.3870e-01    4.0033e+05 ;    C13 - C17
    20     24   1    1.4740e-01    3.0443e+05 ;    C14 - C18
    21     25   1    1.4740e-01    3.0443e+05 ;    C15 - C19
    22     36   1    1.0870e-01    2.8811e+05 ;    C16 - H9
    23     37   1    1.0870e-01    2.8811e+05 ;    C17 - H10
    24     38   1    1.0890e-01    2.8577e+05 ;    C18 - H11
    25     39   1    1.0890e-01    2.8577e+05 ;    C19 - H12
    26     42   1    1.0930e-01    2.8108e+05 ;    C20 - H15
    26     43   1    1.0930e-01    2.8108e+05 ;    C20 - H16
    26     44   1    1.0930e-01    2.8108e+05 ;    C20 - H17
    27     45   1    1.0930e-01    2.8108e+05 ;    C21 - H18
    27     46   1    1.0930e-01    2.8108e+05 ;    C21 - H19
    27     47   1    1.0930e-01    2.8108e+05 ;    C21 - H20

[ pairs ]
;   ai     aj    funct
     1      3      1 ;     O1 - O3
     1      7      1 ;     O1 - C1
     1     22      1 ;     O1 - C16
     1     30      1 ;     O1 - H3
     2      4      1 ;     O2 - O4
     2      8      1 ;     O2 - C2
     2     23      1 ;     O2 - C17
     2     31      1 ;     O2 - H4
     3     10      1 ;     O3 - C4
     3     14      1 ;     O3 - C8
     3     36      1 ;     O3 - H9
     4     11      1 ;     O4 - C5
     4     15      1 ;     O4 - C9
     4     37      1 ;     O4 - H10
     5     16      1 ;     O5 - C10
     5     21      1 ;     O5 - C15
     5     28      1 ;     O5 - H1
     5     29      1 ;     O5 - H2
     5     38      1 ;     O5 - H11
     6     17      1 ;     O6 - C11
     6     20      1 ;     O6 - C14
     6     28      1 ;     O6 - H1
     6     29      1 ;     O6 - H2
```

```
     6     39      1 ;     O6 - H12
     7     18      1 ;     C1 - C12
     7     20      1 ;     C1 - C14
     7     36      1 ;     C1 - H9
     7     38      1 ;     C1 - H11
     8     19      1 ;     C2 - C13
     8     21      1 ;     C2 - C15
     8     37      1 ;     C2 - H10
     8     39      1 ;     C2 - H12
     9     16      1 ;     C3 - C10
     9     17      1 ;     C3 - C11
     9     38      1 ;     C3 - H11
     9     39      1 ;     C3 - H12
    10     22      1 ;     C4 - C16
    10     24      1 ;     C4 - C18
    10     32      1 ;     C4 - H5
    10     34      1 ;     C4 - H7
    11     23      1 ;     C5 - C17
    11     25      1 ;     C5 - C19
    11     27      1 ;     C5 - C21
    11     33      1 ;     C5 - H6
    11     35      1 ;     C5 - H8
    12     14      1 ;     C6 - C8
    12     16      1 ;     C6 - C10
    12     36      1 ;     C6 - H9
    12     40      1 ;     C6 - H13
    12     42      1 ;     C6 - H15
    12     43      1 ;     C6 - H16
    12     44      1 ;     C6 - H17
    13     15      1 ;     C7 - C9
    13     17      1 ;     C7 - C11
    13     37      1 ;     C7 - H10
    13     41      1 ;     C7 - H14
    13     45      1 ;     C7 - H18
    13     46      1 ;     C7 - H19
    13     47      1 ;     C7 - H20
    14     24      1 ;     C8 - C18
    14     30      1 ;     C8 - H3
    14     34      1 ;     C8 - H7
    15     25      1 ;     C9 - C19
    15     31      1 ;     C9 - H4
    15     35      1 ;     C9 - H8
    16     22      1 ;    C10 - C16
    16     30      1 ;    C10 - H3
    16     32      1 ;    C10 - H5
    17     23      1 ;    C11 - C17
    17     31      1 ;    C11 - H4
    17     33      1 ;    C11 - H6
    18     30      1 ;    C12 - H3
    18     32      1 ;    C12 - H5
    19     27      1 ;    C13 - C21
    19     31      1 ;    C13 - H4
    19     33      1 ;    C13 - H6
    20     25      1 ;    C14 - C19
    20     34      1 ;    C14 - H7
    21     24      1 ;    C15 - C18
    21     35      1 ;    C15 - H8
    22     40      1 ;    C16 - H13
    23     41      1 ;    C17 - H14
    24     28      1 ;    C18 - H1
    24     29      1 ;    C18 - H2
    25     28      1 ;    C19 - H1
    25     29      1 ;    C19 - H2
    26     10      1 ;    C20 - C4
    26     18      1 ;    C20 - C12
    32     36      1 ;     H5 - H9
    33     37      1 ;     H6 - H10
    34     38      1 ;     H7 - H11
    35     39      1 ;     H8 - H12

[ angles ]
;   ai     aj     ak    funct   theta         cth
     1     12     10      1    1.1920e+02    5.8400e+02 ;     O1 - C6     - C4
     1     12     18      1    1.1920e+02    5.8400e+02 ;     O1 - C6     - C12
     1     26     42      1    1.0882e+02    4.2543e+02 ;     O1 - C20    - H15
     1     26     43      1    1.0882e+02    4.2543e+02 ;     O1 - C20    - H16
     1     26     44      1    1.0882e+02    4.2543e+02 ;     O1 - C20    - H17
```

```
     2     13     11      1    1.1920e+02    5.8400e+02 ;     O2 - C7     - C5
     2     13     19      1    1.1920e+02    5.8400e+02 ;     O2 - C7     - C13
     2     27     45      1    1.0882e+02    4.2543e+02 ;     O2 - C21    - H18
     2     27     46      1    1.0882e+02    4.2543e+02 ;     O2 - C21    - H19
     2     27     47      1    1.0882e+02    4.2543e+02 ;     O2 - C21    - H20
     3     18     12      1    1.1994e+02    5.8450e+02 ;     O3 - C12    - C6
     3     18     22      1    1.1994e+02    5.8450e+02 ;     O3 - C12    - C16
     4     19     13      1    1.1994e+02    5.8450e+02 ;     O4 - C13    - C7
     4     19     23      1    1.1994e+02    5.8450e+02 ;     O4 - C13    - C17
     5     20      9      1    1.2311e+02    5.6928e+02 ;     O5 - C14    - C3
     5     20     24      1    1.2292e+02    5.7965e+02 ;     O5 - C14    - C18
     6     21      9      1    1.2311e+02    5.6928e+02 ;     O6 - C15    - C3
     6     21     25      1    1.2292e+02    5.7965e+02 ;     O6 - C15    - C19
     7     10     12      1    1.1997e+02    5.6216e+02 ;     C1 - C4     - C6
     7     10     30      1    1.2001e+02    4.0551e+02 ;     C1 - C4     - H3
     7     14     22      1    1.1997e+02    5.6216e+02 ;     C1 - C8     - C16
     7     14     32      1    1.2001e+02    4.0551e+02 ;     C1 - C8     - H5
     7     16     24      1    1.2731e+02    5.3631e+02 ;     C1 - C10    - C18
     7     16     34      1    1.1512e+02    3.9397e+02 ;     C1 - C10    - H7
     8     11     13      1    1.1997e+02    5.6216e+02 ;     C2 - C5     - C7
     8     11     31      1    1.2001e+02    4.0551e+02 ;     C2 - C5     - H4
     8     15     23      1    1.1997e+02    5.6216e+02 ;     C2 - C9     - C17
     8     15     33      1    1.2001e+02    4.0551e+02 ;     C2 - C9     - H6
     8     17     25      1    1.2731e+02    5.3631e+02 ;     C2 - C11    - C19
     8     17     35      1    1.1512e+02    3.9397e+02 ;     C2 - C11    - H8
     9     20     24      1    1.1686e+02    5.2969e+02 ;     C3 - C14    - C18
     9     21     25      1    1.1686e+02    5.2969e+02 ;     C3 - C15    - C19
    10      7     14      1    1.1997e+02    5.6216e+02 ;     C4 - C1     - C8
    10      7     16      1    1.2066e+02    5.4292e+02 ;     C4 - C1     - C10
    10     12     18      1    1.1997e+02    5.6216e+02 ;     C4 - C6     - C12
    11      8     15      1    1.1997e+02    5.6216e+02 ;     C5 - C2     - C9
    11      8     17      1    1.2066e+02    5.4292e+02 ;     C5 - C2     - C11
    11     13     19      1    1.1997e+02    5.6216e+02 ;     C5 - C7     - C13
    12      1     26      1    1.1797e+02    5.2108e+02 ;     C6 - O1     - C20
    12     10     30      1    1.2001e+02    4.0551e+02 ;     C6 - C4     - H3
    12     18     22      1    1.1997e+02    5.6216e+02 ;     C6 - C12    - C16
    13      2     27      1    1.1797e+02    5.2108e+02 ;     C7 - O2     - C21
    13     11     31      1    1.2001e+02    4.0551e+02 ;     C7 - C5     - H4
    13     19     23      1    1.1997e+02    5.6216e+02 ;     C7 - C13    - C17
    14      7     16      1    1.2066e+02    5.4292e+02 ;     C8 - C1     - C10
    14     22     18      1    1.1997e+02    5.6216e+02 ;     C8 - C16    - C12
    14     22     36      1    1.2001e+02    4.0551e+02 ;     C8 - C16    - H9
    15      8     17      1    1.2066e+02    5.4292e+02 ;     C9 - C2     - C11
    15     23     19      1    1.1997e+02    5.6216e+02 ;     C9 - C17    - C13
    15     23     37      1    1.2001e+02    4.0551e+02 ;     C9 - C17    - H10
    16     24     20      1    1.2641e+02    5.3773e+02 ;    C10 - C18    - C14
    16     24     38      1    1.1798e+02    4.2041e+02 ;    C10 - C18    - H11
    17     25     21      1    1.2641e+02    5.3773e+02 ;    C11 - C19    - C15
    17     25     39      1    1.1798e+02    4.2041e+02 ;    C11 - C19    - H12
    18      3     40      1    1.0947e+02    4.0878e+02 ;    C12 - O3     - H13
    18     22     36      1    1.2001e+02    4.0551e+02 ;    C12 - C16    - H9
    19      4     41      1    1.0947e+02    4.0878e+02 ;    C13 - O4     - H14
    19     23     37      1    1.2001e+02    4.0551e+02 ;    C13 - C17    - H10
    20      9     21      1    1.1161e+02    5.3605e+02 ;    C14 - C3     - C15
    20      9     28      1    1.0968e+02    3.9497e+02 ;    C14 - C3     - H1
    20      9     29      1    1.0968e+02    3.9497e+02 ;    C14 - C3     - H2
    20     24     38      1    1.1726e+02    3.8987e+02 ;    C14 - C18    - H11
    21      9     28      1    1.0968e+02    3.9497e+02 ;    C15 - C3     - H1
    21      9     29      1    1.0968e+02    3.9497e+02 ;    C15 - C3     - H2
    21     25     39      1    1.1726e+02    3.8987e+02 ;    C15 - C19    - H12
    22     14     32      1    1.2001e+02    4.0551e+02 ;    C16 - C8     - H5
    23     15     33      1    1.2001e+02    4.0551e+02 ;    C17 - C9     - H6
    24     16     34      1    1.1829e+02    4.1991e+02 ;    C18 - C10    - H7
    25     17     35      1    1.1829e+02    4.1991e+02 ;    C19 - C11    - H8
    28      9     29      1    1.0835e+02    3.2995e+02 ;     H1 - C3     - H2
    42     26     43      1    1.0955e+02    3.2786e+02 ;    H15 - C20    - H16
    42     26     44      1    1.0955e+02    3.2786e+02 ;    H15 - C20    - H17
    43     26     44      1    1.0955e+02    3.2786e+02 ;    H16 - C20    - H17
    45     27     46      1    1.0955e+02    3.2786e+02 ;    H18 - C21    - H19
    45     27     47      1    1.0955e+02    3.2786e+02 ;    H18 - C21    - H20
    46     27     47      1    1.0955e+02    3.2786e+02 ;    H19 - C21    - H20

[ dihedrals ] ; propers
; treated as RBs in GROMACS to use combine multiple AMBER torsions per quartet
;    i      j      k      l   func    C0         C1         C2         C3         C4
C5
```

```
     1     12     10      7      3   30.33400    0.00000  -30.33400    0.00000
0.00000    0.00000 ;     O1-    C6-    C4-    C1
     1     12     10     30      3   30.33400    0.00000  -30.33400    0.00000
0.00000    0.00000 ;     O1-    C6-    C4-    H3
     1     12     18      3      3   30.33400    0.00000  -30.33400    0.00000
0.00000    0.00000 ;     O1-    C6-   C12-    O3
     1     12     18     22      3   30.33400    0.00000  -30.33400    0.00000
0.00000    0.00000 ;     O1-    C6-   C12-   C16
     2     13     11      8      3   30.33400    0.00000  -30.33400    0.00000
0.00000    0.00000 ;     O2-    C7-    C5-    C2
     2     13     11     31      3   30.33400    0.00000  -30.33400    0.00000
0.00000    0.00000 ;     O2-    C7-    C5-    H4
     2     13     19      4      3   30.33400    0.00000  -30.33400    0.00000
0.00000    0.00000 ;     O2-    C7-   C13-    O4
     2     13     19     23      3   30.33400    0.00000  -30.33400    0.00000
0.00000    0.00000 ;     O2-    C7-   C13-   C17
     3     18     12     10      3   30.33400    0.00000  -30.33400    0.00000
0.00000    0.00000 ;     O3-   C12-    C6-    C4
     3     18     22     14      3   30.33400    0.00000  -30.33400    0.00000
0.00000    0.00000 ;     O3-   C12-   C16-    C8
     3     18     22     36      3   30.33400    0.00000  -30.33400    0.00000
0.00000    0.00000 ;     O3-   C12-   C16-    H9
     4     19     13     11      3   30.33400    0.00000  -30.33400    0.00000
0.00000    0.00000 ;     O4-   C13-    C7-    C5
     4     19     23     15      3   30.33400    0.00000  -30.33400    0.00000
0.00000    0.00000 ;     O4-   C13-   C17-    C9
     4     19     23     37      3   30.33400    0.00000  -30.33400    0.00000
0.00000    0.00000 ;     O4-   C13-   C17-   H10
     5     20      9     21      3    0.00000    0.00000    0.00000    0.00000
0.00000    0.00000 ;     O5-   C14-    C3-   C15
     5     20      9     28      3    3.68192   -4.35136    0.00000    1.33888
0.00000    0.00000 ;     O5-   C14-    C3-    H1
     5     20      9     29      3    3.68192   -4.35136    0.00000    1.33888
0.00000    0.00000 ;     O5-   C14-    C3-    H2
     5     20     24     16      3   18.20040    0.00000  -18.20040    0.00000
0.00000    0.00000 ;     O5-   C14-   C18-   C10
     5     20     24     38      3   18.20040    0.00000  -18.20040    0.00000
0.00000    0.00000 ;     O5-   C14-   C18-   H11
     6     21      9     20      3    0.00000    0.00000    0.00000    0.00000
0.00000    0.00000 ;     O6-   C15-    C3-   C14
     6     21      9     28      3    3.68192   -4.35136    0.00000    1.33888
0.00000    0.00000 ;     O6-   C15-    C3-    H1
     6     21      9     29      3    3.68192   -4.35136    0.00000    1.33888
0.00000    0.00000 ;     O6-   C15-    C3-    H2
     6     21     25     17      3   18.20040    0.00000  -18.20040    0.00000
0.00000    0.00000 ;     O6-   C15-   C19-   C11
     6     21     25     39      3   18.20040    0.00000  -18.20040    0.00000
0.00000    0.00000 ;     O6-   C15-   C19-   H12
     7     10     12     18      3   30.33400    0.00000  -30.33400    0.00000
0.00000    0.00000 ;     C1-    C4-    C6-   C12
     7     14     22     18      3   30.33400    0.00000  -30.33400    0.00000
0.00000    0.00000 ;     C1-    C8-   C16-   C12
     7     14     22     36      3   30.33400    0.00000  -30.33400    0.00000
0.00000    0.00000 ;     C1-    C8-   C16-    H9
     7     16     24     20      3   55.64720    0.00000  -55.64720    0.00000
0.00000    0.00000 ;     C1-   C10-   C18-   C14
     7     16     24     38      3   55.64720    0.00000  -55.64720    0.00000
0.00000    0.00000 ;     C1-   C10-   C18-   H11
     8     11     13     19      3   30.33400    0.00000  -30.33400    0.00000
0.00000    0.00000 ;     C2-    C5-    C7-   C13
     8     15     23     19      3   30.33400    0.00000  -30.33400    0.00000
0.00000    0.00000 ;     C2-    C9-   C17-   C13
     8     15     23     37      3   30.33400    0.00000  -30.33400    0.00000
0.00000    0.00000 ;     C2-    C9-   C17-   H10
     8     17     25     21      3   55.64720    0.00000  -55.64720    0.00000
0.00000    0.00000 ;     C2-   C11-   C19-   C15
     8     17     25     39      3   55.64720    0.00000  -55.64720    0.00000
0.00000    0.00000 ;     C2-   C11-   C19-   H12
     9     20     24     16      3   18.20040    0.00000  -18.20040    0.00000
0.00000    0.00000 ;     C3-   C14-   C18-   C10
     9     20     24     38      3   18.20040    0.00000  -18.20040    0.00000
0.00000    0.00000 ;     C3-   C14-   C18-   H11
     9     21     25     17      3   18.20040    0.00000  -18.20040    0.00000
0.00000    0.00000 ;     C3-   C15-   C19-   C11
     9     21     25     39      3   18.20040    0.00000  -18.20040    0.00000
0.00000    0.00000 ;     C3-   C15-   C19-   H12
```

```
    10      7     14     22      3   30.33400    0.00000  -30.33400    0.00000
0.00000    0.00000 ;     C4-    C1-    C8-   C16
    10      7     14     32      3   30.33400    0.00000  -30.33400    0.00000
0.00000    0.00000 ;     C4-    C1-    C8-    H5
    10      7     16     24      3   55.64720    0.00000  -55.64720    0.00000
0.00000    0.00000 ;     C4-    C1-   C10-   C18
    10      7     16     34      3   55.64720    0.00000  -55.64720    0.00000
0.00000    0.00000 ;     C4-    C1-   C10-    H7
    10     12     18     22      3   30.33400    0.00000  -30.33400    0.00000
0.00000    0.00000 ;     C4-    C6-   C12-   C16
    11      8     15     23      3   30.33400    0.00000  -30.33400    0.00000
0.00000    0.00000 ;     C5-    C2-    C9-   C17
    11      8     15     33      3   30.33400    0.00000  -30.33400    0.00000
0.00000    0.00000 ;     C5-    C2-    C9-    H6
    11      8     17     25      3   55.64720    0.00000  -55.64720    0.00000
0.00000    0.00000 ;     C5-    C2-   C11-   C19
    11      8     17     35      3   55.64720    0.00000  -55.64720    0.00000
0.00000    0.00000 ;     C5-    C2-   C11-    H8
    11     13      2     27      3    7.53120    0.00000   -7.53120    0.00000
0.00000    0.00000 ;     C5-    C7-    O2-   C21
    11     13     19     23      3   30.33400    0.00000  -30.33400    0.00000
0.00000    0.00000 ;     C5-    C7-   C13-   C17
    12      1     26     42      3    1.60247    4.80742    0.00000   -6.40989
0.00000    0.00000 ;     C6-    O1-   C20-   H15
    12      1     26     43      3    1.60247    4.80742    0.00000   -6.40989
0.00000    0.00000 ;     C6-    O1-   C20-   H16
    12      1     26     44      3    1.60247    4.80742    0.00000   -6.40989
0.00000    0.00000 ;     C6-    O1-   C20-   H17
    12     10      7     14      3   30.33400    0.00000  -30.33400    0.00000
0.00000    0.00000 ;     C6-    C4-    C1-    C8
    12     10      7     16      3   30.33400    0.00000  -30.33400    0.00000
0.00000    0.00000 ;     C6-    C4-    C1-   C10
    12     18      3     40      3    7.53120    0.00000   -7.53120    0.00000
0.00000    0.00000 ;     C6-   C12-    O3-   H13
    12     18     22     14      3   30.33400    0.00000  -30.33400    0.00000
0.00000    0.00000 ;     C6-   C12-   C16-    C8
    12     18     22     36      3   30.33400    0.00000  -30.33400    0.00000
0.00000    0.00000 ;     C6-   C12-   C16-    H9
    13      2     27     45      3    1.60247    4.80742    0.00000   -6.40989
0.00000    0.00000 ;     C7-    O2-   C21-   H18
    13      2     27     46      3    1.60247    4.80742    0.00000   -6.40989
0.00000    0.00000 ;     C7-    O2-   C21-   H19
    13      2     27     47      3    1.60247    4.80742    0.00000   -6.40989
0.00000    0.00000 ;     C7-    O2-   C21-   H20
    13     11      8     15      3   30.33400    0.00000  -30.33400    0.00000
0.00000    0.00000 ;     C7-    C5-    C2-    C9
    13     11      8     17      3   30.33400    0.00000  -30.33400    0.00000
0.00000    0.00000 ;     C7-    C5-    C2-   C11
    13     19      4     41      3    7.53120    0.00000   -7.53120    0.00000
0.00000    0.00000 ;     C7-   C13-    O4-   H14
    13     19     23     15      3   30.33400    0.00000  -30.33400    0.00000
0.00000    0.00000 ;     C7-   C13-   C17-    C9
    13     19     23     37      3   30.33400    0.00000  -30.33400    0.00000
0.00000    0.00000 ;     C7-   C13-   C17-   H10
    14      7     10     30      3   30.33400    0.00000  -30.33400    0.00000
0.00000    0.00000 ;     C8-    C1-    C4-    H3
    14      7     16     24      3   55.64720    0.00000  -55.64720    0.00000
0.00000    0.00000 ;     C8-    C1-   C10-   C18
    14      7     16     34      3   55.64720    0.00000  -55.64720    0.00000
0.00000    0.00000 ;     C8-    C1-   C10-    H7
    15      8     11     31      3   30.33400    0.00000  -30.33400    0.00000
0.00000    0.00000 ;     C9-    C2-    C5-    H4
    15      8     17     25      3   55.64720    0.00000  -55.64720    0.00000
0.00000    0.00000 ;     C9-    C2-   C11-   C19
    15      8     17     35      3   55.64720    0.00000  -55.64720    0.00000
0.00000    0.00000 ;     C9-    C2-   C11-    H8
    16      7     10     30      3   30.33400    0.00000  -30.33400    0.00000
0.00000    0.00000 ;    C10-    C1-    C4-    H3
    16      7     14     22      3   30.33400    0.00000  -30.33400    0.00000
0.00000    0.00000 ;    C10-    C1-    C8-   C16
    16      7     14     32      3   30.33400    0.00000  -30.33400    0.00000
0.00000    0.00000 ;    C10-    C1-    C8-    H5
    17      8     11     31      3   30.33400    0.00000  -30.33400    0.00000
0.00000    0.00000 ;    C11-    C2-    C5-    H4
    17      8     15     23      3   30.33400    0.00000  -30.33400    0.00000
0.00000    0.00000 ;    C11-    C2-    C9-   C17
```

```
    17      8     15     33      3   30.33400    0.00000  -30.33400    0.00000
0.00000    0.00000 ;    C11-    C2-    C9-    H6
    18     12     10     30      3   30.33400    0.00000  -30.33400    0.00000
0.00000    0.00000 ;    C12-    C6-    C4-    H3
    18     22     14     32      3   30.33400    0.00000  -30.33400    0.00000
0.00000    0.00000 ;    C12-   C16-    C8-    H5
    19     13      2     27      3    7.53120    0.00000   -7.53120    0.00000
0.00000    0.00000 ;    C13-    C7-    O2-   C21
    19     13     11     31      3   30.33400    0.00000  -30.33400    0.00000
0.00000    0.00000 ;    C13-    C7-    C5-    H4
    19     23     15     33      3   30.33400    0.00000  -30.33400    0.00000
0.00000    0.00000 ;    C13-   C17-    C9-    H6
    20      9     21     25      3    0.00000    0.00000    0.00000    0.00000
0.00000    0.00000 ;    C14-    C3-   C15-   C19
    20     24     16     34      3   55.64720    0.00000  -55.64720    0.00000
0.00000    0.00000 ;    C14-   C18-   C10-    H7
    21      9     20     24      3    0.00000    0.00000    0.00000    0.00000
0.00000    0.00000 ;    C15-    C3-   C14-   C18
    21     25     17     35      3   55.64720    0.00000  -55.64720    0.00000
0.00000    0.00000 ;    C15-   C19-   C11-    H8
    22     18      3     40      3    7.53120    0.00000   -7.53120    0.00000
0.00000    0.00000 ;    C16-   C12-    O3-   H13
    23     19      4     41      3    7.53120    0.00000   -7.53120    0.00000
0.00000    0.00000 ;    C17-   C13-    O4-   H14
    24     20      9     28      3    0.00000    0.00000    0.00000    0.00000
0.00000    0.00000 ;    C18-   C14-    C3-    H1
    24     20      9     29      3    0.00000    0.00000    0.00000    0.00000
0.00000    0.00000 ;    C18-   C14-    C3-    H2
    25     21      9     28      3    0.00000    0.00000    0.00000    0.00000
0.00000    0.00000 ;    C19-   C15-    C3-    H1
    25     21      9     29      3    0.00000    0.00000    0.00000    0.00000
0.00000    0.00000 ;    C19-   C15-    C3-    H2
    26      1     12     10      3    7.53120    0.00000   -7.53120    0.00000
0.00000    0.00000 ;    C20-    O1-    C6-    C4
    26      1     12     18      3    7.53120    0.00000   -7.53120    0.00000
0.00000    0.00000 ;    C20-    O1-    C6-   C12
    32     14     22     36      3   30.33400    0.00000  -30.33400    0.00000
0.00000    0.00000 ;     H5-    C8-   C16-    H9
    33     15     23     37      3   30.33400    0.00000  -30.33400    0.00000
0.00000    0.00000 ;     H6-    C9-   C17-   H10
    34     16     24     38      3   55.64720    0.00000  -55.64720    0.00000
0.00000    0.00000 ;     H7-   C10-   C18-   H11
    35     17     25     39      3   55.64720    0.00000  -55.64720    0.00000
0.00000    0.00000 ;     H8-   C11-   C19-   H12

[ dihedrals ] ; impropers
; treated as propers in GROMACS to use correct AMBER analytical function
;    i      j      k      l   func   phase     kd      pn
     1     12     18     10      1   180.00   4.60240   2 ;     O1-    C6-   C12-    C4
     7     12     10     30      1   180.00   4.60240   2 ;     C1-    C6-    C4-    H3
     7     22     14     32      1   180.00   4.60240   2 ;     C1-   C16-    C8-    H5
     7     24     16     34      1   180.00   4.60240   2 ;     C1-   C18-   C10-    H7
     8     13     11     31      1   180.00   4.60240   2 ;     C2-    C7-    C5-    H4
     8     23     15     33      1   180.00   4.60240   2 ;     C2-   C17-    C9-    H6
     8     25     17     35      1   180.00   4.60240   2 ;     C2-   C19-   C11-    H8
     9     24     20      5      1   180.00  43.93200   2 ;     C3-   C18-   C14-    O5
     9     25     21      6      1   180.00  43.93200   2 ;     C3-   C19-   C15-    O6
    10     14      7     16      1   180.00   4.60240   2 ;     C4-    C8-    C1-   C10
    11     15      8     17      1   180.00   4.60240   2 ;     C5-    C9-    C2-   C11
    11     19     13      2      1   180.00   4.60240   2 ;     C5-   C13-    C7-    O2
    12     22     18      3      1   180.00   4.60240   2 ;     C6-   C16-   C12-    O3
    13     23     19      4      1   180.00   4.60240   2 ;     C7-   C17-   C13-    O4
    14     18     22     36      1   180.00   4.60240   2 ;     C8-   C12-   C16-    H9
    15     19     23     37      1   180.00   4.60240   2 ;     C9-   C13-   C17-   H10
    20     16     24     38      1   180.00   4.60240   2 ;    C14-   C10-   C18-   H11
    21     17     25     39      1   180.00   4.60240   2 ;    C15-   C11-   C19-   H12
```

CURRICULUM VITAE

Personal Information

Name and surname : Mahdi Ibrahim SAEED

Nationality : Iraq

Birthplace and Date : Duhok/Iraq, 1975

Telephone : +964 750 496 3856

Email : mahdiworld3gmail.com

Education

Degree	Institution	Year of Graduation
High school	: Duhok	1997
Bachelor's Degree	: Department of Physics at College of Science, Duhok University, Iraq	2001
MS Degree	: Department of Physics at Siirt University Institute of Science, Turkey	2018

Research Interests

Physical, Theoretical and Computational Chemistry, Biophysical Chemistry

Foreign Language

English, Arabic, Turkish